**Responses to review comments 2:**

AC: The authors would like to thank anonymous Reviewer 2 for the time taken to comment on our manuscript and provide the helpful suggestions listed below. We have addressed each comment and where we have been unable to implement the recommended amendments, we have provided an explanation as to why. The revised manuscript is much improved, especially the supplementary section which has been rewritten following the feedback provided from both reviewers. The review comments are listed here in italics and preceded by “RC” and the authors’ response in regular font preceded by “AC”.

*RC: The study “Improving Antarctic Bottom Water precursors in NEMO for climate applications” by Katherine Hutchinson and colleagues is an exciting demonstration on feasibility and importance of including ice shelf–ocean interaction in coarse resolution (1˚), global ocean and climate models. Over the past two decades a growing body of literature has documented the processes of ice melt in ice shelf cavities around Antarctica, their implications on water mass transformation and modelling approaches thereof. It is an ongoing debate, how this is best implemented in coarse resolution models used for multi-centennial climate simulations. Hutchinson et al. show that even on a 1˚ ocean model grid one can include and simulate the three largest Antarctic ice-shelf cavities interactively using complex physic.*

*The manuscript is well written and composed, the arguments supported by mostly clear and matching figure. It would be desirable though if the authors could provide a little more background in the introduction on modelling approaches for ice shelf melt and ice cavity circulation, reference early studies such as Hellmer (2004, doi:10.1029/2004GL019506) and other approaches like the PICO model (Reese et al., 2018, doi:10.5194/tc-12-1969-2018), just to name a couple of examples. By the way, Hellmer 2004 is listed as reference but not cited in the main text. Introduction and discussion are sufficient to introduce the subject and to validate the results but do not really reach beyond. The authors make a great effort to properly validate their simulations, clearly state weaknesses of their model (and its strengths) but also where observations are sparse and thus differences may not necessarily mean a model bias.*

AC: Thank you for bringing it to our attention that more context regarding approaches to modeling ice shelf melt could be useful. The authors decided to not do an extensive literature review on all the other models simulating sub ice shelf cavity circulation because it is a study in and of itself and to do so comprehensively would be its own review article. Instead we present a summary of all models using NEMO. To satisfy this review comment we have added the following to the introduction:

“The simulations with a fixed freshwater flux parameterization at depth perform well in terms of mimicking the vertical overturning and associated entrainment of ice shelf melt, but do not allow for interactive ice-ocean exchange that evolves with ocean properties. Parameterizations of ice shelf melt using far field temperature (outside of the cavities) exist and an extensive comparison was undertaken in Burgard et al. (2022). Here they found that none of the available parameterizations yield a negligible error, and so parameterizing basal melt still remains a challenge. Furthermore, these parameterizations do not solve the need to allow for circulation underneath the ice shelves in order to produce the horizontal variability observed on the continental shelf. For this, it is necessary to open the sub-ice shelf cavities in the simulation (Mathiot et al., 2017; Storkey et al., 2018; Comeau et al., 2022) ”

Please note Hellmer et al., (2004) is listed in Table 1 summarizing the net melt rates for various ice shelves. That is why the reference is in the bibliography even though it is not directly cited in the main text.

*RC: The authors provide bathymetry and initial conditions used for the ice shelf cavities along with some simulation output, which is very much appreciated. Information missing but likely of interest to the community would be the additional computational effort caused by including, “opening” the cavities.*

AC: Thank you for pointing this out, yes this information is useful. We have added to following line to the methodology: “In terms of computing cost, the “Open” cavity configuration costs 11% more than the “Closed” cavity simulation (mostly due to addition of cells as the model grid is extended further south; only 0.3% of this is associated with the cost of the ice shelf routines themselves)”.

*RC: While the manuscript overall is strong and certainly merits publication with GMD being a very suitable journal, I see three weak spots that could be revised prior to publication:*

*1) Arguments are typically well made and supported throughout the text. Only towards the end of subsection 4.4 and in subsection 4.5 the text makes the impression that the authors want to address the given topics but the text is rather short, referring to several supplementary figures (e.g., lines 494-501) without really being able to pinpoint the interaction with open ocean deep convection and sea ice and the role of the ASC.*

AC:

We appreciate the reviewer raising this as the sea ice supplementary material was added shortly before submission and, indeed, improvements can be made. The sea ice supplement went into a level of detail and was not needed for this study and so the validation against observations has been removed and will be the focus of a separate study. Supplementary Section S3 (“An evaluation of sea ice production and polynya activity in the NEMO simulations”) has been revised and re-focused, and the following text has been added to the end of subsection 4.4 to summarize the relevant sea ice production findings:

“ High ice production is seen on the southwest continental shelves of the Weddell and Ross Seas in Supplementary Figs. S2a and S2b. Opening the cavities slightly reduces the magnitude of ice production in the Ronne Depression (Fig. S2c) and at the location of the Terra Nova Bay Polynya (Fig. S2d) and increases the production of ice further east. There is no overall change in the principal location of polynya activity and the slight west/east decrease/increase in sea ice is presumed to have a negligible effect on the total amount of HSSW generated. As such, the reduction of the highly saline HSSW signature seen in Figs. 2g and 3g when cavities are opened is likely due to a conversion to ISW (and not from a decrease in HSSW production itself). Please see the Supplementary Information Sect. 3 for an evaluation of simulated polynyas near the studied ice shelves and a diagnosis on the effect of opening the cavities on ice production.”

RC: *A particular issue is that in the “Open” case one can see an offshore displacement of the deep convection region (Fig. S2e) but not really an overall weakening/shoaling, which seems to contradict studies simulating ice-shelf melt impacts by freshwater release (Beadling et al., 2022, doi:10.1029/2021JC017608; Bronselaer et al., 2018, doi:10.1038/s41586-018-0712-z). The authors show that the ASC is weak in their simulation, which would rather facilitate a freshening of the interior Weddell Gyre and hence decrease MLD. Please discuss.*

AC: The MLD figure which was in Supplementary material has been moved into the main text and is now Fig. 8. The following paragraph has been added to the end of Section 4:

“Once a model is able to explicitly form the parent waters of AABW in the right locations on the continental shelf (and export this dense water), it will become necessary for modelers to tone-down open ocean deep convection as this workaround will be longer relied upon to form the totality of AABW. Here we explore the impact that opening the cavities has on MLD to diagnose the extent of vertical convection in the model. Some reduction in MLD is seen on the continental shelf and slope in the Filchner (Fig. 8e) and Challenger Troughs (Fig. 8f) due to the increase in stratification as a result of the greater bottom densities associated with outflowing ISW (Fig. S4a and S4c). The presence of ISW appears to promote slightly increased ice production in these areas, as discussed earlier. In this case, it is therefore the ocean properties that drive sea ice and the brine rejection associated with elevated ice production is found to have a minor effect on water properties. Within the region of exaggerated MLDs off the Weddell continental slope, the MLDs deepen in the “Open” cavity experiment (positive anomalies Figs. 8e). We hypothesise that this deepening is associated with an overall cooling of the subsurface layers due to a horizontal mixing of ISW, unimpeded by a relatively weak and diffuse Antarctic Slope Current (discussed in the following section). Overall, in wintertime, mixed layers are on average 19 m deeper over the whole Weddell Sea region in the “Open” cavity experiment compared to the reference “Closed” simulation. This reinforcement of the high MLD bias highlights the need for work to be done on reducing wintertime deep convection, together with better representing dense water overflows”

RC: *2) Section 5, the discussion mostly reads like a summary and I suggest to actually rename the section accordingly ("Summary and Discussion"). This is okay as the model results are intensively discussed and validated already in Sections 3 and 4, which reach beyond the typical presentation of results. In addition, results of other modelling approaches could be discussed, like with the UKESM (Smith et al., 2021, already cited) or the PICO model mentioned above. This would be particularly helpful as the authors use a forced ocean model but understand their study as a contribution to improving climate models as they state in the introduction.*

AC:

Done, section re-named "Summary and Discussion".

As for comparison with other model results: We actually struggled to find similar studies where the effects of opening the cavities in a global NEMO configuration were compared extensively and validated against observations. For example, while the paper of Smith et al. (2021) goes to great effort to document the technical steps undertaken to couple the ocean and ice-shelves, it does not explore impact on water masses. We do directly compare our results with Bull et al (2021) and Hausmann et al. (2019) which are respectively 1/4° and 1/12° configurations of NEMO for the Weddell Sea with open sub-ice shelf cavities. In fact Figure 5 is designed to match the aspect and colorbars of Bull et al. (2021) Figure 4 to facilitate easier comparison. As for a discussion on other coupled climate model results, we summarize the net melt rates in Table 1 but have decided that it is out of scope in this paper to embark on a detailed literature review on all forced and coupled ocean models who simulate sub-ice shelf cavity simulation. We feel this would dilute the focus of the paper.

RC: *3) The sea ice production and polynya activity analysis in the supplementary material goes to some length but without clear results. There is no significant difference in sea ice production due to opening the cavities (table S1) except the discussed spatial displacements. The latter are rather simple responses to changes in surface water mass properties. The authors should be careful not to contradict arguments made in the main text and overinterpret the role of sea ice. This seems to be the case in the summary section S1.6, where in particular references to figures of bottom(!) salinity (Figs. 2i, 3i) are more confusing than supportive.*

AC: Thank you for raising this. The sea ice supplementary material has been completely revised and is now better aligned with the main text. Please see Supplementary Section 3.

RC: *The list of references needs to be properly checked for consistency.*

AC: The references have been checked again, thank you for flagging this.

RC: *While extensive, all comments are rather minor and should be addressible without requiring an additional round of review.*

AC: Thank you for the time taken to provide this valuable feedback.

RC:

*Minor comments by line:*

*Line 1, the title: I wish "by opening ice shelf cavities" would somehow be included. The formulation "AABW precursors" appears kind of indirect and less appealing to me -- though less technical, I admit.*

AC: This was debated amongst the authors before initial submission and as only the 3 sub-ice shelf cavities thought to play major roles in the formation of AABW parent waters were opened, we wanted to state this clearly in the title. "By opening ice shelf cavities" could be misleading by insinuating that all cavities are open, which they are not.

RC: *l.33: add references like Fröhlicher et al. (2015, doi:10.1175/JCLI-D-14-00117.1) and maybe Bourgeois et al. (2022, doi:10.1038/s41467-022-27979-5) and*

AC: Frölicher et al. (2015) is found to be relevant and has been added. Thank you for the recommendation.

RC: *l.35-38: introductions of both HSSW and ISW could use a reference each where the interested reader could find more detail on formation processes*

AC: Indeed, references to Jenkins (1991) and Jacobs et al. (1979) have been added.

RC: *l.175-177 details of sea ice advection scheme etc. is provided here. Please provide similar information on ocean model in prev. paragraph. Focus is the ocean model.*

AC: A section has been added in supplementary material (S1) explaining the ocean model namelists with reference to the NEMO manual.

RC: *l.187, 199, etc: term "cold-core ice shelves" or "cold ice shelves" needs introduction or at least a reference; maybe in addition refer to "dense shelf" as defined in Thompson et al. (2018, doi:10.1029/2018RG000624)*

AC: This expression has been amended to 'cold water' and 'cold cavities' to be clearer and in line with existing nomenclature.

RC: *Section 2.4 The entire approach of attaining the initial conditions is wonderful, very thoughtful and a great example. I would be curious though, how much the model state still* *drifts in the ice shelf cavities after starting the main 100+ year long run. Could be added to the supplementary.*

AC: Indeed, it would be useful to quantify whether the model retains information from initialization after a few decades. Unfortunately, performing such an assessment is not possible with the present 124 year run as we force it with 2 consecutive cycles of CORE atmospheric conditions that include interannual and longer-term variability (related to climate change). In order to have access to model drift, we should run a long simulation forced by climatological present-day conditions, which we have not done so far. This is work that is being considered for future investigation.

RC: *l.241 and 251: Figure S3 is addressed before S2. Switch figures in supplementary.*

AC: Figure S2 has been moved into the main text and is now Figure 8, Figure S3 has now become S2.

RC: *l.303: add "ice shelf" in "The average ice shelf melt rate pattern …"*

AC: Added.

RC: *l.313: careful with the resolution statement. I assume the earlier studies use NEMO3.x and potentially also different settings complicating a direct comparison.*

AC: Correct, both these studies use older versions of NEMO. The impact on model results delivered by improvements in functionality in NEMO are, however, minor compared to the impact of moving from a 1° to a 1/12° resolution. Nevertheless, the statement only mentions "possible impact" and highlights the fact that these are regional configurations thereby explaining that a direct comparison is, of course, not possible. We are simply stating that of the other studies mentioned in the table, as these are both based on NEMO, they are the most relevant to compare eORCA1 with (within reason).

RC: *Table 1: this is an awesome overview, excellent!*

AC: Thank you!

RC: *l.325f add information on figure number in Rignot et al and Haussmann et al.*

AC: This has been added, thank you.

RC*: l.348 & 370: drop subsection header; subsections consist of 1 paragraph each only.*

AC: Okay, they have been removed.

RC: *l.362 remind the reader here that eORCA1, i.e. 1 degree, in fact means 22km actual resolution*

AC: This has been edited to read: “It is therefore encouraging that eORCA1 (with an effective horizontal resolution under FRIS of 22 km) captures these, as they could play an important role in the evolution of shelf circulation in future climate scenarios (Naughten et al., 2021).”

RC: *l.403f & 416f: please provide an average difference estimate for “fresher, slightly cooler” and “cooler fresher values”*

AC: The following has been updated: “A change in signature of AABW can, however, be seen in the volumetric T-S plot (Supplementary Material Fig. S3a), where explicit ocean-ice shelf interaction results in a small shift in volume towards cooler fresher AABW (Open - Closed weighted average shift in AABW volume by -0.008 °C and -0.003 psu).”

And: “The volumetric T-S plot for the Ross Sea found in Supplementary Material (Fig. S3b) indicates that opening the RIS cavity has moved the core of AABW towards slightly cooler fresher values, accompanied by a 0.34 % decrease in volume of AABW as defined by the original water mass limits (delineated in green in Fig. S3b; Open - Closed weighted average shift in AABW volume by -0.001 °C and -0.005 psu).”

AC: *l.437: MCDW, abbreviation is not introduced*

AC: Corrected

RC: *l.498: Figures 8 and 9 are only properly introduced in line 525; referring to their panels (d) is more confusing than helpful here*

AC: This paragraph has been re-written and reference to Figures 8 and 9 is now later in the next, after they have been introduced.

RC: *l.528, “little indication of a coherent cascading”: cascading is a rapid process, is it possible that the time mean over 10 years masks such process?*

AC: While in other places the downslope flow of dense water is intermittent and extremely difficult to observe, adjacent to the large ice shelves of the Weddell and Ross Seas, the dense water overflows are considered to be large-scale, highly active and to permanently contribute to AABW formation (Ivanov et al., 2003). The cascading of dense water from the Filcher and Challenger troughs are both considered “active” cascades by Baines and Connie (1998) as they were directly observed by summertime CTD sampling (Foldvok et al., 1985; Jacobs, 1991).

To clarify this in the text, the relevant references have been added.

RC: *l.551: please also reference Colombo et al. (2020, doi:10.5194/gmd-13-3347-2020) on overlow in z-coordinates in NEMO*

AC: This reference has been added.

SUPPLEMENTARY TEXT

RC: *l.929: "An evaluation of sea ice production …" (not to confuse ice shelves and sea ice)*

AC: Corrected

RC: *l.933ff: rewrite: "Sea ice growth, melt and transport exert an influence on water mass properties. Polynyas are large areas of open water or very thin ice forced by local winds or heat from the ocean. Near the Ronne and Ross ice shelf margins, large polynyas source dense saline waters to the surface ocean during the cold season."*

AC: This section has been completely re-written..

RC: *l.948f: rewrite: "… concentration outputs, of which the 2003-2009 average in the is displayed in Figs. S3b and S4b for the "Closed" simulation."*

AC: This section has been completely re-written.

RC: *l.1018 & 1020: you refer to temperature and salinity, which are shown in panels (h) & (i) in Figures 2 and 3 (not only panel (i)).*

AC: This section has been re-written and now refers only to salinity..

FIGURES

RC: *Figure 1: switch panels (a) and (b) as Weddell Sea (currently panel b) is addressed first in the text. Also, please increase line thickness of the circulation arrows for visibility.*

AC: This has been done.

RC: *Figure 2 (and all other contour/pcolor plots): use discrete colors and fewer color levels (max. 20 or even only 10) often help to improve readability of the graphic.*

AC: The authors understand this point and have discussed it. We have used cmocean to plot all temperature and salinity plots as this package is standard and fit-for-purpose having oceanographic specific colorbars for "thermal" and "haline". Unfortunately cmocean functionality is fixed as being perceptually uniform, and so it is not possible to split the colorbars into discrete intervals. Doing so would require a change of colormap, and the authors feel that this would be a greater disservice to readability than having perceptually uniform colorbars.

For more information on the cmocean toolbox please refer to: Thyng, Kristen, et al. “True Colors of Oceanography: Guidelines for Effective and Accurate Colormap Selection.” Oceanography, vol. 29, no. 3, The Oceanography Society, Sept. 2016, pp. 9–13, doi:10.5670/oceanog.2016.66.

RC: *Further, please increase line thickness of the gray dashed line of freezing point (panels a,d,g).*

AC: This has been done.

RC: *Caption: add “of WOA and “Closed” after “…bottom temperature and salinity” in line 272. And add last “Panels (a) and (g) exclude ice shelf cavity data matching the “Closed” configuration of panel (d).” (as stated later in line 388)*

AC: Thank you for these suggestions, the caption has been amended accordingly.

RC: *Figure 4: panels should have some location (lat/lon) or distance labelling along frame.*

AC: This has been done.

RC: *Figure 5a: velocity arrows are way too small, reduce number and increase length and thickness; also red arrows on green shading is not color-blind friendly, black arrows would do*

AC: This has been done.

RC: *Figure S1, caption: mention that scatter dots are placed in T-S space according to “Closed” and coloring shows “Open”-“Closed”; also this should be Figure 3 according to the sequence in which supplementary figures are addressed in the main text*

AC: The caption has been amended accordingly.

# Improving Antarctic Bottom Water precursors in NEMO for climate applications

Katherine Hutchinson [1], Julie Deshayes [1], Christian Éthé [1], Clément Rousset [1], Casimir de Lavergne [1], Martin Vancoppenolle [1], Nicolas C. Jourdain [2], and Pierre Mathiot [2]

[1] LOCEAN Laboratory, Sorbonne Université CNRS-IRD-MNHN, Paris, France
[2] Univ. Grenoble Alpes/CNRS/IRD/G-INP, IGE, Grenoble, France

*Correspondence to*: Katherine Hutchinson (kath.hutchinson@gmail.com)

**Abstract.** The world's largest ice shelves are found in the Antarctic Weddell and Ross Seas where complex interactions between the atmosphere, sea ice, ice shelves and ocean transform shelf waters into High Salinity Shelf Water (HSSW) and Ice Shelf Water (ISW), the parent waters of Antarctic Bottom Water (AABW). This process feeds the lower limb of the global overturning circulation as AABW, the world's densest and deepest water-mass, spreads outwards from Antarctica. None of the coupled climate models contributing to CMIP6 directly simulated ocean-ice shelf interactions, thereby omitting a potentially critical piece of the climate puzzle. As a first step towards better representing these processes in a global ocean model, we run a 1° resolution forced configuration of NEMO (eORCA1) to explicitly simulate circulation beneath Filchner-Ronne (FRIS), Larsen C (LCIS), and Ross (RIS) ice shelves. These locations are thought to supply the majority of the source waters for AABW and so melt in all other cavities is provisionally prescribed. Results show that the grid resolution of 1° is sufficient to produce melt rate patterns and ~~net~~total melt ~~rates~~fluxes of FRIS (117 ± 21 Gt/yr), LCIS (36 ~~+~~± 7 Gt/yr) and RIS (112 ~~+~~± 22 Gt/yr) that agree well with both high resolution models and satellite measurements. Most notably, allowing sub-ice shelf circulation reduces salinity biases (0.1 psu), produces the previously unresolved water mass ISW, and re-organises the shelf circulation to bring the regional model hydrography closer to observations. A change in AABW within the Weddell and Ross Seas towards colder, fresher values is identified but the magnitude is limited by the absence of a realistic overflow. This study presents a NEMO configuration that can be used for climate applications with improved realism of the Antarctic continental shelf circulation and a better representation of the precursors of AABW.

**Plain language summary.** Bottom Water constitutes the ~~lower limb~~bottom half of the ocean's overturning system and is primarily formed in the Antarctic Weddell and Ross Seas due to interactions between the atmosphere, ocean, sea ice and ice shelves. Here we use a global ocean 1° resolution model with explicit representation of the three large ice shelves important for the formation of the parent waters of Bottom Water~~ explicitly represented and~~. We find doing so reduces ~~salinity~~salt biases, improves water mass realism, and gives realistic ice shelf melt rates.

**Style Definition:** Bullets: Outline numbered + Level: 1 + Numbering Style: 1, 2, 3, … + Start at: 1 + Alignment: Left + Aligned at: 0 cm + Tab after: 1.27 cm + Indent at: 1.27 cm

## 1 Introduction

The Southern Ocean plays a vital role in global ocean circulation and in the storage of both heat and carbon (Marshall and Speer, 2012; Frölicher et al., 2015; Rintoul, 2018). Within this backdrop, the processes taking place adjacent to and underneath the Antarctic ice shelves are not only important for controlling regional ocean dynamics but also for facilitating globally important water mass transformations (Schodlok et al., 2015). Sea ice formation on the continental shelf decreases the buoyancy of the underlying waters through the process of brine rejection creating High Salinity Shelf Water (HSSW~~).~~; Jacobs et al., 1979). When this dense water mass is formed adjacent to an ice shelf, it can follow deep bathymetric pathways into the ~~neighboring~~neighbouring sub-ice shelf cavity and interact with the base of the ice to form Ice Shelf Water (ISW; Jenkins, 1991). These dense waters then accumulate on the continental shelf and migrate towards the shelf break to cascade down the continental slope as a gravity current (Gordon, 1986; Whitehead, 1987). As the waters descend towards the depths, they mix with and entrain ambient water masses until they reach either a density neutral depth, or the sea floor, at which point they spread outwards as Antarctic Bottom Water (AABW) (Bergamasco et al., 2003; Huthnance 1995). AABW plays a crucial role in the global overturning circulation, in abyssal ventilation and in the cross-basin transport of heat, salt, carbon, nutrients and numerous other tracers (Killworth, 1983; Johnson, 2008; Orsi, 2010). The principal locations for the formation of the source waters of AABW are the Weddell and Ross Seas adjacent to the large ice shelves (Orsi et al., 1999; van Caspel et al., 2015; Kerr et al., 2018; Bowen et al., 2021).

Filchner Ronne Ice Shelf (FRIS) is located at the southern boundary of the Weddell Sea and represents 28% of the total Antarctic ice shelf area (Fig. ~~1b~~1a). Traditionally FRIS has been viewed as having the greatest contribution to AABW by forming the coldest and most oxygen-rich dense waters in the Southern Ocean (Nicholls et al., 2009; Naveira Garabato et al., 2002). Observations for the southern Weddell Sea continental shelf indicate that HSSW enters the FRIS cavity following the Ronne Depression (Fig. ~~1b~~1a), circulates under the cavity causing melting at the base of the ice shelf at great water pressures and then exits as colder and fresher ISW via the Filchner Trough (Nicholls et al., 2001; Nicholls et al., 2004; Janout et al, 2021). This outflowing ISW mixes with HSSW formed on the shallow continental shelf adjacent to Berkner Island and cascades down the continental slope, mixing with ambient modified Circumpolar Deep Water (CDW) to form AABW (Fahrbach et al., 1995; Nicholls et al., 2009).

While the main formation site of the source waters of AABW in the Weddell Sea is the FRIS continental shelf, Larsen-C Ice Shelf (LCIS) is also thought to play an important role. Nestled into the arc of the Antarctic Peninsula (Fig. ~~1b~~1a), processes adjacent to this ice shelf produce a fresher variety of dense water called Weddell Sea Deep Water (WSDW), which is lighter than the Weddell Sea Bottom Water (WSBW) formed further south (Fahrbach et al., 1995; Gordon et al., 2001). This water mass is less hindered by bathymetric constraints so that it is more easily transported out of the gyre over the South Scotia Ridge to make ~~a valuable~~an important contribution to AABW (Abrahamsen et al., 2019; van Caspel et al., 2015).

The Ross Sea, the second largest site for AABW formation, is home to Antarctica's largest ice shelf representing 32 % of the total Antarctic ice shelf area (Rignot et al., 2013). The Ross Ice Shelf (RIS) is located at the southern boundary of the Ross Sea (Fig. ~~1a~~1b) where the continental shelf has very irregular topography with numerous troughs and depressions that act as reservoirs for dense waters (Budillon et al., 2003). Just offshore, CDW flows largely un-modified within the Ross Gyre and mixes with the local waters at the shelf break (Fig. ~~1a~~1b), providing a source of heat and making this a region of dynamic water mass exchange (Bergamasco et al., 2003; Budillon et al., 2003). Two recurring ice-free zones are the principal formation sites for HSSW in the area: one located at the south-western corner of the Ross Sea called the Terra Nova Bay polynya and another in front of RIS called the Ross Sea Polynya. This HSSW then spreads both northwards towards the shelf break and southwards under RIS (Fig. ~~1a~~1b). Similarly to FRIS, the HSSW flowing into the RIS cavity interacts with the base of the ice shelf to form ISW (Jacobs et al., 1979).

While freshwater input to the ocean from ice shelf melt is (at present) relatively small in magnitude, it exerts a strong modulating effect on dense water formation and Southern Ocean water mass transformation (Schodlok et al., 2015; Jeong et al., 2020). The impacts of increased meltwater in a warming climate could, in addition to raising sea level, actually reduce AABW formation with major consequences for global overturning (Silvano et al., 2018~~).~~, Williams et al., 2016). One possible series of events common to simulations by the E3SM, CSIRO Mk3L and LOVECLIM climate models describes how surface freshening from ice shelf melt would increase stratification along the Antarctic coast, inhibit full depth convection and the formation of dense shelf water, and simultaneously trap warm water at depth resulting in further ice shelf melting and a horizontal propagation of the warming signal (Jeong et al., 2020; Phipps et al., 2016; Menviel et al., 2010).

Despite the importance of ocean-ice shelf interactions for the climate system, none of the models contributing to the DECK experiments of the Coupled Model Intercomparison Project Phase 6 (CMIP6, used to inform the Intergovernmental Panel on Climate Change (IPCC) assessment report 6 (AR6)) explicitly represented circulation within sub-ice shelf cavities (Heuze et al., 2021). This has lowered confidence in projected trends for the Southern Ocean and has limited our ability to incorporate the impacts of global ocean warming on the Antarctic Ice Sheet (Meredith et al., 2019; Beadling et al., 2020; Comeau et al., 2022). In most coupled climate models, the formation of dense water is poorly represented as AABW is formed via open ocean convection, often with mixed layers that are too deep, and polynyas that are too large and too frequent (Heuze et al., 2013; Mohrmann et al., 2021). In reality, deep open-ocean convection events able to produce AABW are rarely observed (Goosse et al. 2021) and instead ocean–sea-ice–atmosphere interactions adjacent to the Antarctic ice shelves are responsible for the creation of the majority of AABW source waters.

The authors propose that the path towards improving AABW realism in coupled climate models starts with a more accurate simulation of the dense precursors on the Antarctic continental shelf. Then, work needs to be done on improving the overflows so as to facilitate the downslope export of these waters, and on decreasing the strength of open ocean convection (Heuze et al., 2021). The Nucleus for European Modelling of the Ocean (NEMO) model is used as the ocean component in many climate models (Hazeleger et al., 2010; Scoccimarro et al., 2011; Hewitt et al., 2011, 2016; Dufresne et al., 2013; Voldoire et al., 2013; Cao et al., 2018; Swart et al., 2019) and consequently the development of configurations with improved realism of Antarctic shelf water circulation and AABW source water properties is of interest to a large community.

Ice shelf melt has previously been represented using NEMO in a variety of ways: prescribed using a freshwater flux at the surface, a fixed flux distributed over the depth range of the mouth of the ice shelf front, a specified melt at the base of the ice shelf, and an interactive melt with both fixed geometry and evolving coupled ice shelves (Mathiot et al., 2017; Storkey et al., 2018; Smith et al., 2021). The simulations with a fixed freshwater flux ~~parameterisation~~parameterization at depth perform well in terms of mimicking the vertical overturning and associated entrainment of ice shelf melt~~. This representation, however, is limited by its inability to produce the horizontal variability observed adjacent to large ice shelves and it does~~, but do not allow for interactive ice-ocean exchange that evolves with ocean properties. ~~For this, it is necessary to~~ Parameterizations of ice shelf melt using far field temperature (outside of the cavities) exist and an extensive comparison was undertaken in Burgard et al. (2022). Here they found that none of the available parameterizations yield a negligible error, and so parameterizing basal melt still remains a challenge. Furthermore, these parameterizations do not solve the need to allow for circulation underneath the ice ~~shelf~~ shelves in order to produce the horizontal variability observed on the continental shelf. For this, it is necessary to open the sub-ice shelf cavities in the simulation (Mathiot et al., 2017; Storkey et al., 2018; Comeau et al., 2022). Of all the previous studies using NEMO configurations with explicit sub-ice shelf cavities, only one has been at a resolution that is compatible with long-term climate projection applications, that developed by Smith et al. (2021) where a global ocean 1° NEMO (eORCA1) is coupled with interactive ice sheets in the the U.K. Earth System model (UKESM). Previous studies have proven very useful in illustrating the strengths and weaknesses of NEMO's representation of ocean-ice shelf interactions but the results apply to regional configurations (e.g. Mathiot et al., 2017; Jourdain et al., 2017; Hausmann et al., 2020; Huot et al. 2021) or high resolution global configurations (e.g. 1/4° and 1/12° in Storkey et al., 2018) and so do not fit the needs of typical CMIP models. The results presented by Smith et al. (2021) for UKESM with NEMO eORCA1 coupled to an Antarctic ice sheet model highlight the substantial advancement in model development, but do not show how this coupling affects the realism of Southern Ocean water mass properties and dynamics. Evaluation of the initial state of the UKESM (NEMO coupled to BICYCLES ice sheet model) was undertaken by Siahaan et al. (2021), but the investigation served to check for the absence of large biases and so an in-depth comparison was not carried out.

A gap therefore exists to take a step-by-step approach to represent ice shelf-ocean interactions in NEMO for climate applications. Additionally, a well documented description of one possible method to simulate sub-ice shelf cavity circulation in low resolution ocean models could be of use in the designing of the next phase of CMIP. In this study we present the first proposed step in this journey by explicitly simulating circulation under only Ross Ice Shelf (RIS), Filchner-Ronne Ice Shelf (FRIS) and Larsen C Ice Shelf (LCIS). ~~We choose to keep all other ice shelves closed with prescribed melt rates injected at the mouth of the front using the method described by Mathiot et al. (2017).~~ RIS, FRIS and LCIS were chosen due to their direct role in the formation ~~and setting of properties~~ of the parent waters of AABW (Kerr et al., 2018; Bowen et al., 2021), and due to their large size and thus practicality of realistically simulating their sub-ice shelf cavities in a global ocean 1° setup. We choose to keep all other ice shelf cavities closed with prescribed melt rates injected at the mouth of the front using the method described by Mathiot et al. (2017). This includes the relatively large Amery Ice Shelf cavity, despite its role in preconditioning bottom water formation in the Cape Darnley polynya (Williams et al., 2016), because this polynya is absent in our configuration (due to the absence of icebergs and landfast sea ice). We choose to explore the changes in circulation, melt rates, and water mass properties in the Weddell and Ross Seas in a forced scenario with fixed cavity geometry, as coupling can introduce further biases and obscure the changes attributed to sub-ice shelf circulation. By taking this circumspect approach it is possible to diagnose the impact of ocean-ice shelf interactions on the parent waters of AABW and produce a validated configuration of NEMO that can either be used for the next generation of climate models or as an interim step towards dynamic ice-sheet coupling.

The model setup, configurations used in this study, forcing, and methodology to establish initial conditions under the ice shelves are described in Sect. 2. A validation of the reference configuration compared to ocean observations is presented in Sect. 3. Sect. 4 then explores the results from the "Open" cavity simulation and compares melt rates and thermohaline properties with other model estimates and observed values. Sect. 5 provides the reader with a summary discussion, and Sect. 6 presents a conclusion of the findings of this study. Additional information regarding model namelist nomenclature, representation of tides, an investigation into sea ice~~,~~ production, and plots showing AABW volume and bottom density changes ~~along with an analysis of mixed layer depths in the model compared to an observational atlas~~ are provided in Supplementary Material.

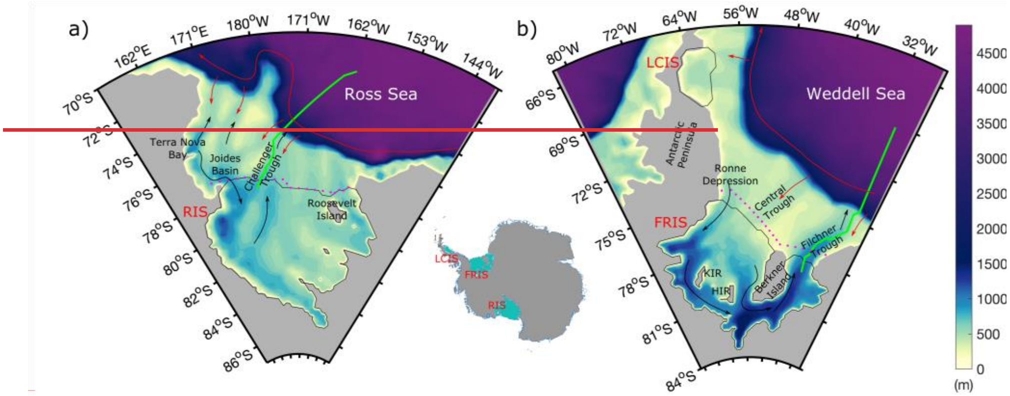

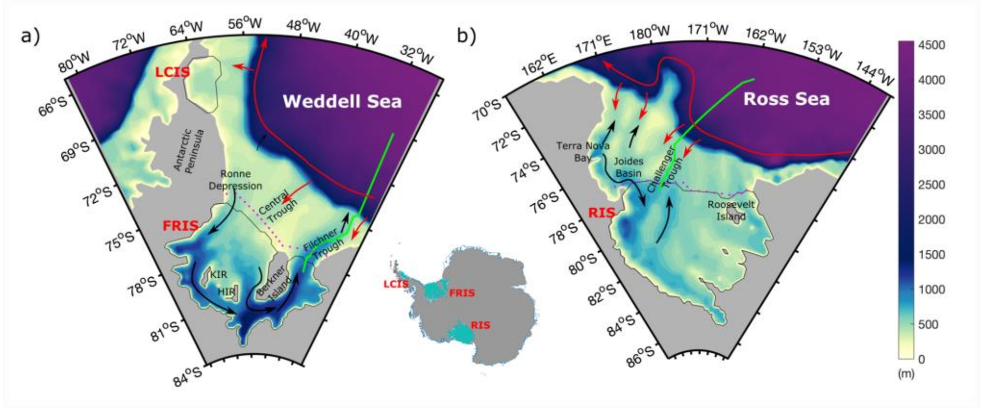

Figure 1: Model bathymetry for (a) the ~~Ross~~Weddell and (b) ~~Weddell~~Ross Seas with main topographic features labeled (KIR: Korff Ice Rise; HIR: Henry Ice Rise). Red arrows show direction of flow of warm deep water and black arrows indicate dense shelf water circulation according to observational estimates. Circulation features depicted in this figure are adapted from information presented in Budillon et al. (2003), Bergamasco et al. (2003), Russo et al. (2011) and Janout et al. (2018). Magenta dotted lines indicate sections used for CTD comparisons and green lines show shelf cross sections used for analysis in Figs. ~~8~~6 and ~~9~~7.

## 2 Methods

### 2.1 Model setup

For this study, we use version 4.2 of NEMO ~~is used~~ (NEMO System Team, 2022). NEMO is a three-dimensional, free-surface, hydrostatic, primitive-equation global ocean general circulation model. Our configuration uses the eORCA1 global grid with nominal horizontal resolution of 1° at the equator and a reduction in meridional grid spacing towards higher latitudes to match the accompanying shrinking of the zonal dimension of the grid cells. In the Southern Hemisphere, the model grid has been extended to reach 85° S to allow for the representation of the sub-ice shelf seas according to the procedure described in Mathiot et al. (2017). The average horizontal resolution of the grid under RIS, FRIS, and LCIS is 20 km, 22 km and 42 km respectively. To account for the decrease in the horizontal size of grid cells at high latitudes, we decide to linearly scale ~~horizontal~~the laplacian eddy viscosity south of 65° S according to grid cell size. In the vertical, the configuration possesses 75 levels, with thickness increasing from 1 m at the surface to 200 m at depth (Storkey et al., 2017). We use the z* vertical coordinate adapted to the ice shelf so that all cells between the surface and the ice shelf base are masked at initialisation and the effect of the ice shelf on friction and pressure gradient is calculated (Madec and NEMO ~~team, 2016~~System Team, 2019; Mathiot et al., 2017). The bathymetry used is derived from the ~~ETOPO2v2~~Earth TOPOgraphy version 2 data set (ETOPO2v2; NOAA, 2006) with information for the extension under the ice shelves based on the International Bathymetric Chart of the Southern Ocean (IBSCO~~ (~~; Arndt et al., 2013). For the calculation of the thermodynamic properties of seawater, NEMO uses the Thermodynamic Equation Of Seawater - 2010 (TEOS-10) giving results in conservative temperature and absolute salinity, which for the purposes of this study, were converted to potential temperature and practical salinity in order to facilitate comparison of the model results with observations and known signatures of water masses. For more information regarding the choices of advection and diffusion schemes, mixing coefficients, and eddy parameterizations, please refer to the copy of the namelists provided in the accompanying data repository. ~~–~~A note explaining the nomenclature of the namelists and the differences between the “Open” and “Closed” cavity simulations can be found in Supplementary Material Sect. S1.

The effect of tides on vertical mixing (through breaking of internal waves) is taken into account in NEMO using the energy constrained parameterization of de Lavergne et al. (2020). This mixing parameterization does not, however, represent trapped waves at high latitudes or any tide-induced internal-wave mixing below ice shelves, and does not include the effect of tides on basal friction and thus melting of the ice shelves. To address this, by default there is a parameter (rn_ke0) representing the background kinetic energy associated with tides which is set to a constant of 2.5 x 10-3 m2 s-2 everywhere. We tested another methodology of parameterizing the impact of tides on melting according to Jourdain et al. (2019) using CATS2008 two-dimensional tidal velocities; as summarised in Supplementary Material Sect. S2 and Fig. S1, this alternative parameterization brings marginal changes in the simulated melt patterns and bulk melt rates (< 10 %). The explicit representation of tides is not advisable in a configuration designed for climate applications due to the high levels of numerical mixing induced.

The ocean dynamics component, NEMO OCE, is coupled with SI$^3$, the dynamic and thermodynamic sea ice model of NEMO (Rousset et al., 2015; Vancoppenolle et al., 2023). SI$^3$ is directly resolved on the ocean grid, based on an energy- and salt- conserving approach for sea ice thermodynamics (Vancoppenolle et al., ~~2009~~2023), multiple categories to resolve subgrid scale variations in ice thickness (Bitz et al., 2001; Lipscomb, 2001), a second-order moment-conserving scheme for horizontal advection (Prather, 1986), and the adaptive elastic-viscous-plastic formulation for the rheology term of the momentum equation (Kimmritz et al., 2016).

## 2.2 Open vs Closed Configurations

~~Results~~Here, we present results from two configurations~~ are presented here~~: first a “Closed” cavity reference configuration where ice shelf melt is prescribed in a way ~~to mimic~~that mimics the ice-shelf overturning, and secondly an “Open” cavity configuration. For the reference “Closed” cavity configuration, a fixed freshwater flux corresponding to the volume of basal meltwater estimated by Depoorter et al. (2013) for each ice shelf is added into the ocean evenly between the ocean floor and the base of the ice shelf~~ at the location of~~, horizontally uniform across the ice shelf front, and a vertical wall closes the cavity at this location (as in Mathiot et al., 2017). The fixed freshwater flux is based on Depoorter et al. (2013) melt estimates as this is the same file used for the IPSL climate model. Furthermore, the ice shelf area surveyed by Adusumilli et al. (2020) only extends to 81.5 °S so that RIS and FRIS are not fully covered and therefore don't have the full melt flux. For the “Open” cavity configuration, the majority of ice shelves are kept closed using the same method as described above and only three of the largest cold~~-core~~ water ice shelves are opened. Circulation is simulated under RIS, FRIS and LCIS where the prescribed freshwater flux is turned off at the mouths of these cavities and interactive melt is activated. Ice shelf melt and freeze are calculated using the 3-equation formulation (Hellmer and Olbers, 1989; Holland and Jenkins, 1999; Asay-Davis et al., 2016) in which the temperature, salinity and velocities are averaged over a fixed boundary layer thickness of ~~30m (~~(30 m chosen according to Losch~~,~~ (2008). The top drag coefficient used is $10^{-3}$ and the temperature and salinity transfer coefficients used are $1.4 \times 10^{-2}$ and $4 \times 10^{-4}$ respectively. Note that a fixed ice shelf geometry is maintained, thereby assuming a steady-state where all ice melted by the ocean is replaced by the seaward advection of new ice (Schodlok et al., 2015; Mathiot et al., 2017).

By using this combination of explicit and ~~parameterised~~parameterized ice shelf cavities, we provide an intermediate step between prescribed melt and explicit cavities or even ice sheet coupling, and gain experience and a better understanding of the impact on ocean dynamics in order to better inform future choices. The advantage of this approach is that it allows us to specify the melt for small cavities which remain unresolved or insufficiently resolved at a 1° resolution, and simultaneously utilize the model capability to resolve sub-ice shelf cavity circulation under the large cold ice shelves, which allows for more realistic formation of the source waters of AABW. In terms of computing cost, the “Open” cavity configuration costs 11% more than the “Closed” cavity simulation (mostly due to addition of cells as the model grid is extended further south; only 0.3% of this is associated with the cost of the ice shelf routines themselves). Figure 1 shows the extended bathymetry of eORCA1 for the Weddell and Ross seas with the three ice shelf cavities of interest un-masked and important features ~~labeled~~labelled.

## 2.3 Forcing

For both “Open” and “Closed” configurations, the model was run for 124 years using 2 cycles of interannual (1948-2009) CORE forcing (Coordinated Ocean - ice Reference Experiments version 2; Large & Yeager, 2004; Griffies et al., 2009). Sea surface salinity restoring is activated, but not under sea ice as we have low confidence in the sea surface salinity climatology in this area due to limited observations. Freshwater discharge from iceberg melt is parameterized using a prescribed surface flux with realistic distribution (Merino et al., 2016~~)~~), based on calving estimates from Depoorter et al. (2013).

## 2.4 Initial conditions

For all simulations, global ocean properties were initialized using the 1981-2010 climatology of World Ocean Atlas 2013 (WOA2013; Locarnini et al., 2013; Zweng et al., 2013~~).~~) as this dataset is used for the IPSL climate model and so was a convenient choice. This climatology does not, however, extend under the Antarctic ice shelves and so in order to provide somewhat realistic initial conditions underneath FRIS, LCIS, and RIS, we employed an idealized regional configuration of each ice shelf. For this we created a NEMO test case using a closed domain, with temperature and salinity restoring at the boundaries, 75 vertical layers and a resolution, timestep and bathymetry corresponding to that of eORCA1. The domain for each of the 3 configurations included just the ice shelf and adjacent continental shelf and slope and so were reasonably low-cost and fast to run in order to perform sensitivity experiments. The simulations were initialized with a constant and uniform temperature and salinity and restored at the boundaries using a mean profile from WOA2013 for that region. The choices for initial thermohaline properties inside the cavities were informed by calculating the mean ~~properties~~values of detected ISW from CTD observations performed in the area adjacent to each ice shelf and converting these to conservative temperature and absolute salinity for input to the model ~~(-~~[-2 °C and 34.76 for FRIS (Janout et al., 2021), -1.95 °C and 34.74 for LCIS (Nicholls et al., 2004; Hutchinson et al., 2020), and -1.94 °C and 34.76 for RIS (Bergamasco et al., 2003; Budillon et al., 2003~~).~~)]. Each simulation was run for 10 years, which was found to be sufficiently long to spin-up the circulation within each cavity and reach a stable melt rate. The temperature-salinity distributions within the cavity were extracted and merged with ~~WOA~~WOA2013 data re-gridded to the NEMO eORCA1 grid, with a cubic spline used to smooth the data discontinuity across the ice shelf front. By following this method we have attempted to provide as realistic initial conditions for eORCA1 as possible with the simulation starting with CORE forcing from the 1st of January 1948.

## 3 Water mass realism in NEMO without cavities

To assess the existing biases in the representation of dense water properties in NEMO v4.2 eORCA1 standard configuration (“Closed”), full depth temperature versus salinity plots along with bottom temperature and salinity are compared with World Ocean Atlas (WOA 2018) gridded observations from 1981-2010 (Locarnini et al., 2018; Zweng et al., 2019) in Figs. 2 and 3 for the Weddell and Ross Seas, respectively.

WOA observations indicate the presence of HSSW on the south-western continental shelf of the Weddell Sea, possessing salinities of up to 34.9 psu, likely sourced from the coastal polynya along the western flank of FRIS ice shelf front (~~Figs. 2a, 2c and~~ Supplementary Material Fig. ~~S3a~~S2a). On the eastern side of the FRIS ice shelf front, evidence of ISW can be seen with temperatures below surface freezing point (-1.9 °C) and fresher salinities of around 34.65 psu (Figs. ~~2a~~2b and ~~2b~~2c). Results from CTD observations obtained on the continental shelf in front of FRIS propose a counter-clockwise circulation pattern with HSSW entering the cavity via the Ronne Depression and ISW exiting via the Filchner Trough (Fig. ~~1b~~1a; Janout et al., 2021). By comparison, the standard model configuration is overall too salty on the continental shelf with HSSW properties that are out of the bounds of the observed range (HSSW box Fig. 2d). Most notably, there is a pool of HSSW that has built up in the Ronne Depression resulting in overestimations of bottom salinity and exaggerated cool conditions on the southwestern Weddell shelf (Figs. 2e and 2f). In terms of ISW, there is none detected in the model output (ISW box Fig. 2d~~)~~), as in this configuration there is no explicit ocean-ice shelf interaction. Offshore bottom temperature is overall colder than in WOA, resulting in a core AABW signature that is at the lower limit of observed values (Fig. 2d). This is indicative of the effects of strong open ocean deep convection (Heuze et al., 2021) which is ~~highlighted in Supplementary Fig. S2c by the over-deep mixed layers in the central Weddell Gyre~~discussed further in Sect. 4.4.

Due to the limited observations adjacent to LCIS, WOA bottom properties do not capture the cold water masses located on the continental shelf detected by Hutchinson et al. (2020), where bottom temperatures of below -2 °C and salinities of 34.6 psu were reported. Instead Fig. 2b indicates very warm conditions (temperatures of around 0.5°C) on the western flank of the Weddell Sea. The authors explored the bottom properties in this area in the Southern Ocean State Estimate (SOSE; Mazloff et al., 2010) atlas and found bottom temperatures on the shelf adjacent to LCIS in line with those reported from hydrographic observations (-2 °C) but the bottom salinities were found to be far too fresh (34.5 psu). A fair comparison can therefore not be realistically made between NEMO and an atlas for the area adjacent to LCIS, but by comparing the model output with the CTD results from Hutchinson et al. (2020; their Fig. 3b~~)~~), we find the “Closed” configuration to be too saline with bottom salinities (34.8 psu) greater than that observed. The overly saline conditions along the western flank of the Weddell Sea are likely a spill-over effect from the HSSW buildup seen in the Ronne Depression further south (Fig. 2f).

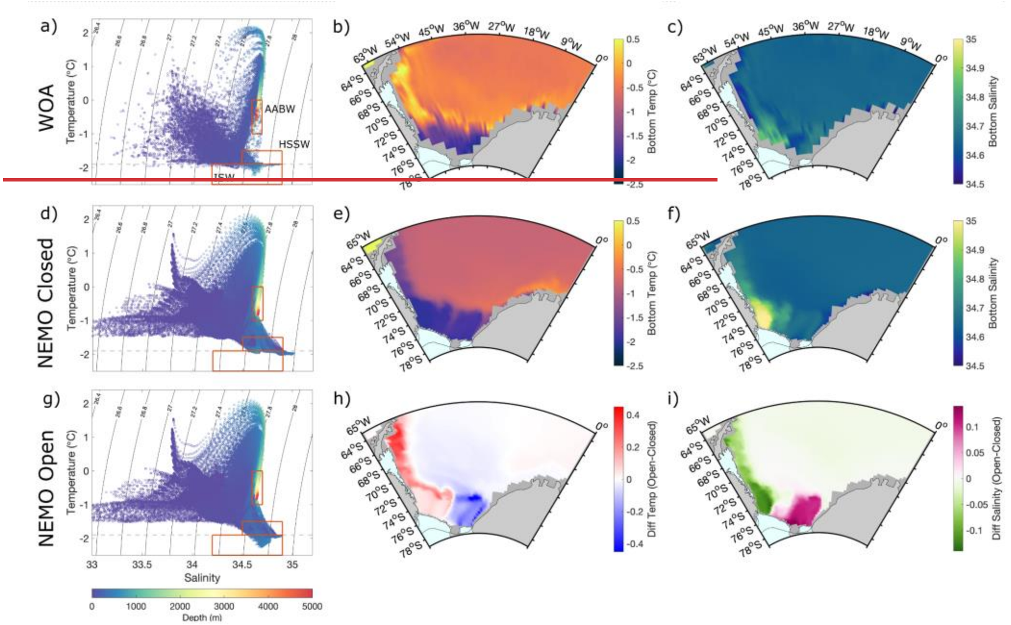

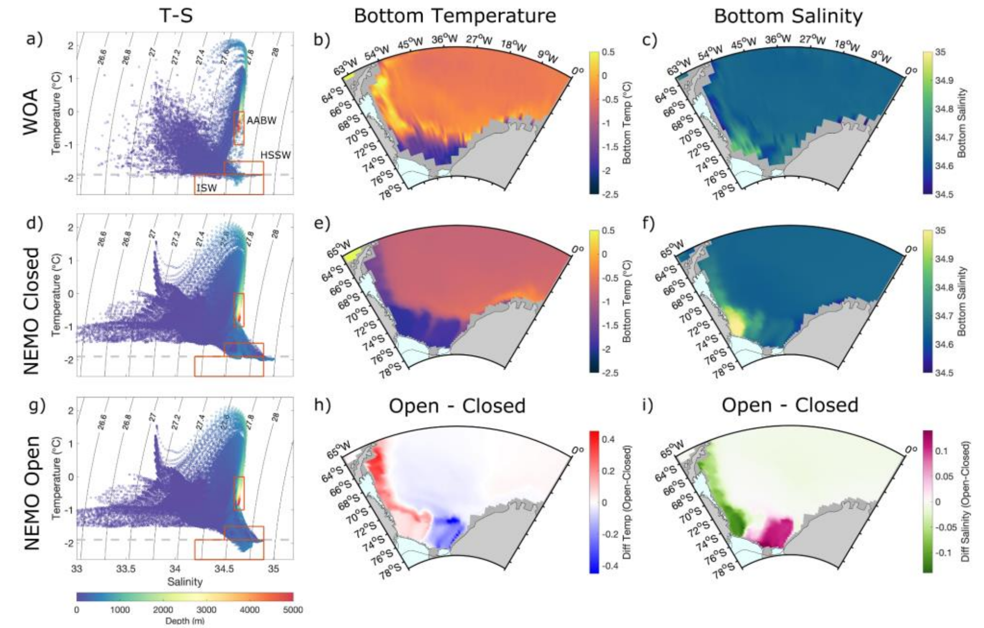

Figure 2: Weddell Sea comparison of NEMO v4.2 eORCA1 reference configuration ( “Closed”; subplots d-f) for equivalent years 1981-2009 to be compared with World Ocean Atlas (WOA; Locarnini et al., 2018; Zweng et al., ~~2018~~2019) observational dataset (subplots a-c). The temperature salinity-distributions in density space are shown in plots (a), (d) and (g) with the dashed gray line representing surface freezing point and labels in plot (a) indicating the observed ranges for properties corresponding to Antarctic Bottom Water (AABW), High Salinity Shelf Water (HSSW) and Ice Shelf Water (ISW) (Robertson et al., 2002; Hutchinson et al., 2020). Plots (b), (c), (e) and (f) show bottom temperature and salinity~~,~~ of WOA and “Closed”, and the difference in bottom properties between the “Open” and “Closed” cavity configurations (Open - Closed) are shown in subplots (h) and (i). Panels (a) and (g) exclude ice shelf cavity data matching the “Closed” configuration of panel (d).

WOA bottom ~~temperature~~temperatures and salinities for the Ross Sea indicate a strong east-west gradient in properties across the continental shelf (Figs. 3b and 3c). Conditions in the south west reveal the cold and salty signature of HSSW likely formed in the Terra Nova Bay polynya and the Ross Polynya. Intrusions of CDW at the eastern portion of the RIS front can be seen by warm signatures of up to 1 °C (~~Figs. 3a and~~Fig. 3b) and fresher bottom salinities (Fig. 3c). Hydrological and current meter data presented by Budillon et al. (~~2011~~2003) reported that HSSW dominates bottom properties within the troughs connected to the Joides Basin, and ISW dominates in the Challenger Trough (see locations of bathymetric features in Fig. ~~1a)~~1b), thus indicating a western intensified anticlockwise circulation cell under RIS. In terms of HSSW properties, the model is within the observed range (Fig. 3d~~)~~), yet the proportion and salinity of HSSW in Terra Nova Bay and Joides Basin

~~appears~~appear to be overestimated (Fig. 3f). The bottom temperatures from NEMO indicate the presence of very warm waters, likely of circumpolar origin right on the eastern continental shelf (Fig. 3e) whereas in observations this shelf is found to be cold and the warm water confined offshore of the shelf break with only occasional intrusions (Bergamasco et al., 2003; Fig. 3b). Again, there is no ISW in this standard configuration, as there is no explicit model representation of ice shelf-ocean interactions. Offshore bottom properties are slightly cooler than WOA in the model, but the AABW signature (AABW box Fig. 3d) falls within the range reported from observations (Bergamasco et al., 2002; Bouillon et al., 2011; Silvano et al., ~~2020).~~

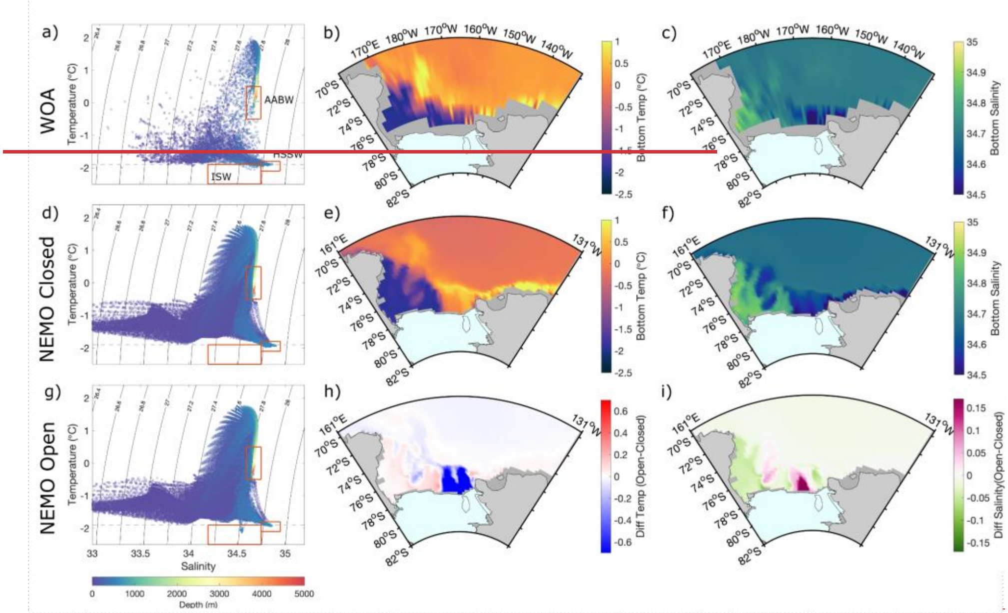

2016).

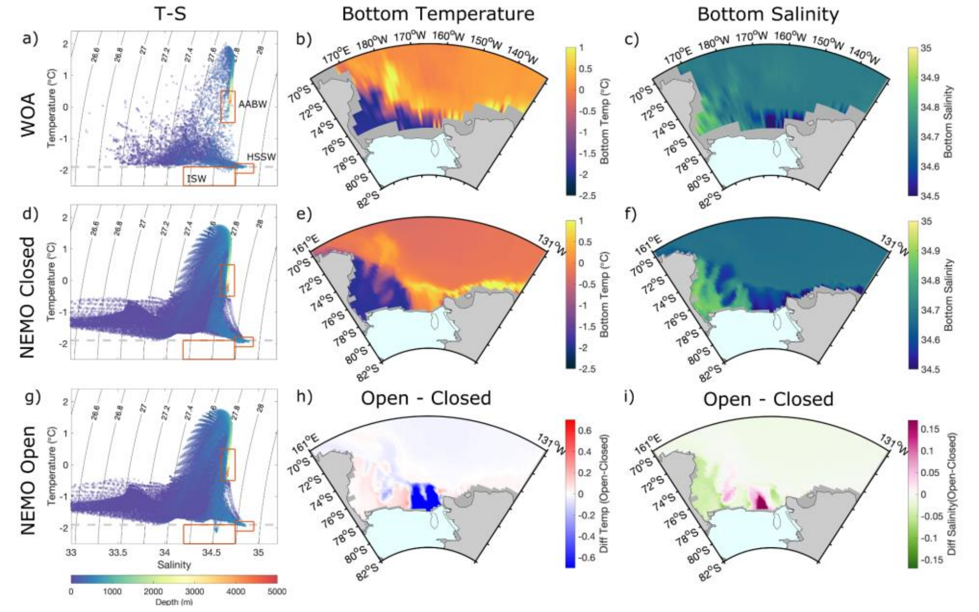

Figure 3: Same as Fig. 2 but for the Ross Sea.

## 4 Impact of explicit sub-ice shelf circulation

The following sections present results pertaining to the “Open” cavity run where the eORCA1 grid is extended under FRIS, LCIS and RIS to allow for circulation within the cavities and explicit interaction with the base of these ice shelves.

### 4.1 Melt rates

The average ice shelf melt rate pattern for FRIS, LCIS and RIS is shown in Fig. 4 for the model simulation equivalent years 1995 to 2009, where orange indicates melt and purple shows refreezing. The average ~~net~~total melt ~~rate~~flux for this time period is shown in Table 1 and compared to Depoorter et al. (2013) from which the volumes for the prescribed melt ~~rates~~ were taken for the reference configuration (“Closed”). Opening the cavities results in at least double the melt reported from Depoorter et al. (2013). This discrepancy reflects both a warm bias on the continental shelf in NEMO (Sect. 4.4) and a possible bias in Depoorter's estimates which are lower than all other satellite estimates (Table 1). The ~~net~~total melt ~~rates~~fluxes of each ice shelf from various other observational and model studies are also listed in the table showing the wide spread in basal melt estimates both within values calculated from observations and between observations and models (Table

1). The model studies of Mathiot et al. (2017) and Bull et al. (2021), which are both regional NEMO 1/4° configurations, and the NEMO 1/12° configuration of the southwestern Weddell Sea of Haussmann et al. (2020), are particularly relevant to compare eORCA1 with, as here we see the possible impact of lowering the resolution in NEMO. For the Weddell Sea, our global 1° (eORCA1) compares well with these regional high resolution studies producing a net basal melt within 12 Gt/yr of the other estimates for FRIS and LCIS. The eORCA1 melt rate for RIS, while~~ being~~ higher than observational studies, is in the middle of other model estimates, and is especially well aligned with that of NEMO 1/4° from Mathiot et al. (2017). Overall, eORCA1's ~~net~~total melt ~~rates~~fluxes correspond well with the average from all other estimates and are well within the standard deviations (last line of Table 1).

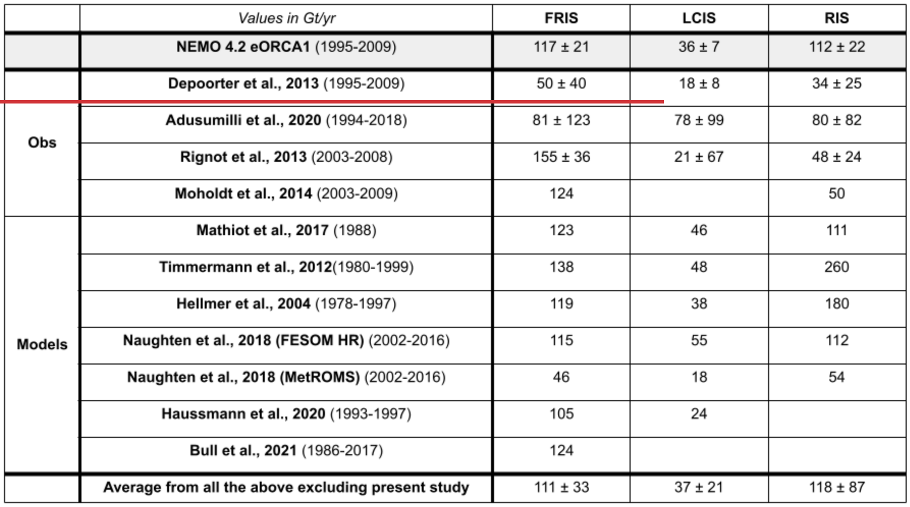

| | *Values in Gt/yr* | **FRIS** | **LCIS** | **RIS** |
|---|---|---|---|---|
| | **NEMO 4.2 eORCA1** (1995-2009) | 117 ± 21 | 36 ± 7 | 112 ± 22 |
| **Obs** | **Depoorter et al., 2013** (1995-2009) | 50 ± 40 | 18 ± 8 | 34 ± 25 |
| | **Adusumilli et al., 2020** (1994-2018) | 81 ± 123 | 78 ± 99 | 80 ± 82 |
| | **Rignot et al., 2013** (2003-2008) | 155 ± 36 | 21 ± 67 | 48 ± 24 |
| | **Moholdt et al., 2014** (2003-2009) | 124 | | 50 |
| **Models** | **Mathiot et al., 2017** (1988) | 123 | 46 | 111 |
| | **Timmermann et al., 2012**(1980-1999) | 138 | 48 | 260 |
| | **Hellmer et al., 2004** (1978-1997) | 119 | 38 | 180 |
| | **Naughten et al., 2018 (FESOM HR)** (2002-2016) | 115 | 55 | 112 |
| | **Naughten et al., 2018 (MetROMS)** (2002-2016) | 46 | 18 | 54 |
| | **Haussmann et al., 2020** (1993-1997) | 105 | 24 | |
| | **Bull et al., 2021** (1986-2017) | 124 | | |
| | **Average from all the above excluding present study** | 111 ± 33 | 37 ± 21 | 118 ± 87 |

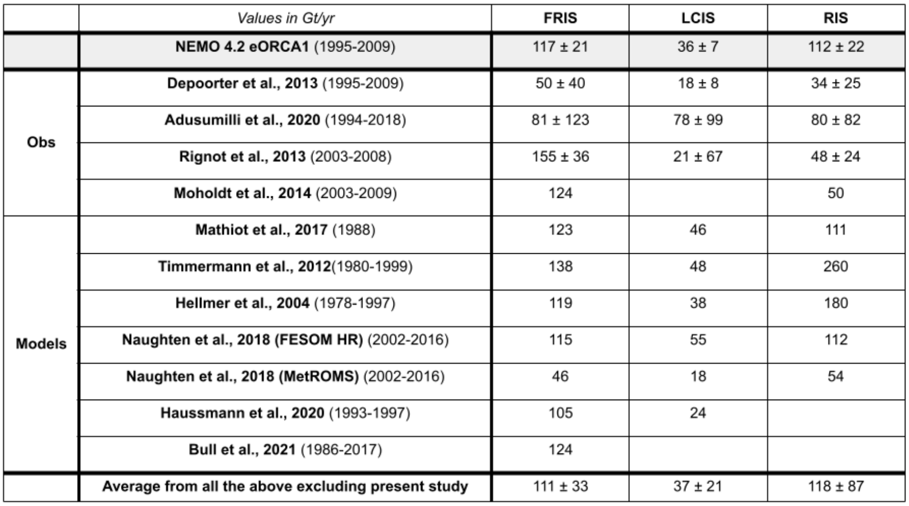

| | *Values in Gt/yr* | **FRIS** | **LCIS** | **RIS** |
|---|---|---|---|---|
| | **NEMO 4.2 eORCA1** (1995-2009) | 117 ± 21 | 36 ± 7 | 112 ± 22 |
| **Obs** | **Depoorter et al., 2013** (1995-2009) | 50 ± 40 | 18 ± 8 | 34 ± 25 |
| | **Adusumilli et al., 2020** (1994-2018) | 81 ± 123 | 78 ± 99 | 80 ± 82 |
| | **Rignot et al., 2013** (2003-2008) | 155 ± 36 | 21 ± 67 | 48 ± 24 |
| | **Moholdt et al., 2014** (2003-2009) | 124 | | 50 |
| **Models** | **Mathiot et al., 2017** (1988) | 123 | 46 | 111 |
| | **Timmermann et al., 2012**(1980-1999) | 138 | 48 | 260 |
| | **Hellmer et al., 2004** (1978-1997) | 119 | 38 | 180 |
| | **Naughten et al., 2018 (FESOM HR)** (2002-2016) | 115 | 55 | 112 |
| | **Naughten et al., 2018 (MetROMS)** (2002-2016) | 46 | 18 | 54 |
| | **Haussmann et al., 2020** (1993-1997) | 105 | 24 | |
| | **Bull et al., 2021** (1986-2017) | 124 | | |
| | **Average from all the above excluding present study** | 111 ± 33 | 37 ± 21 | 118 ± 87 |

Table 1: Comparison of mean ~~net~~total melt ~~rates~~flux (Gigatons per year) for Filchner-Ronne (FRIS), Larsen C (LCIS) and Ross Ice Shelves (RIS) for observational and model studies. The mean and standard deviation of all the estimates depicted in the table excluding the current study are shown at the bottom.

The patterns of melt shown in Fig. 4 also compare well with those of observational estimates like Rignot et al. (2013; their Figure 1) and high resolution model results like Haussmann et al. (2020; their Figure 3) whose color bar we replicated for ease of cross-comparison. If we look at the melt pattern of FRIS and compare it with these two aforementioned studies, we see that eORCA1 captures the high melt rates at the western portion of the ice shelf front, at the southern edge of Berkner Island and along the grounding line at the back of the cavity. The model also correctly simulates the region of refreezing along the western boundary of the circulation cell within the cavity, in both the Ronne and Filchner depressions and the re-freezing in the shallow region between the Korff and Henry Ice Rises (Fig. 4a, see bathymetry location in Fig. ~~1b~~1a). For LCIS, the entire shelf shows a positive melt (Fig. 4b). Observations from Rignot et al. (2013) and simulations from Harrison et al. (2022) indicate some re-freezing under this ice shelf but the regional high resolution model studies of Mathiot et al. (2017) and Haussmann et al. (2020) similarly show melting only. The pattern for RIS generally compares well with that reported from observations but the magnitude of melt at the ice shelf front, especially to the east, is elevated (Fig. 4c).

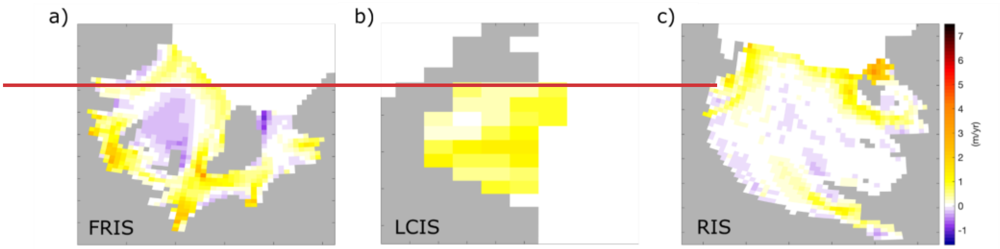

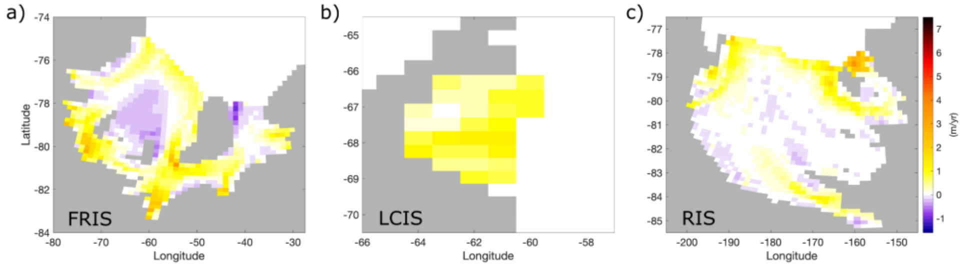

Figure 4: Melt rates in meters per year for (a) Filchner-Ronne Ice Shelf, (b) Larsen C Ice Shelf and (c) Ross Ice Shelf where orange indicates melt and purple re-freezing. The results are mean values for the model equivalent period 1995-2009.

## 4.2 Circulation and properties

Opening the sub-ice shelf cavities in eORCA1~~,~~ allows for the establishment of a horizontal gyre circulation within the cavity and on the continental shelf of the Weddell and Ross Seas, in line with previous studies (Losch et al., 2008; Mathiot et al., 2017).

### ~~4.2.1 FRIS~~

The mean state of circulation from the last 10 years of simulation within the FRIS cavity, along with the associated bottom thermohaline properties can be seen in Figs. 5a-5d. The circulation patterns shown here are in good agreement with Bull et al. (2021) at 1/4° and with Hausmann et al. (~~2019~~2020) at 1/12° with the exception of higher bottom salinities in eORCA1 and a slightly weaker barotropic circulation strength. Note that here we use potential temperature and practical salinity so as to be in line with the other figures of this paper, so approximately 0.17 psu must be added when juxtaposing with absolute salinity plots. The depth averaged velocity and barotropic circulation pattern in Figs. 5a and 5b both indicate an anticlockwise circulation under the ice shelf. Comparatively warm and salty HSSW enters via the Ronne Depression, circulates from west to east, ~~melting~~melts the base of the ice shelf mostly along the grounding line (cold, fresh signatures in Figs. 5c and 5d), and exits via the Filchner Trough as ISW. This pattern is consistent with observations (Nicholls et al., 2001;

Janout et al., 2021). Two pathways of Modified ~~Warm~~Circumpolar Deep Water (~~MWDW~~MCDW) towards the ice shelf front can be seen, both in the circulation pattern (Fig. 5a) and via the bottom temperature (Fig. 5c): one located in the middle of the continental shelf (Central Trough) and the other on the shelf to the east of Filchner Trough. These pathways provide a conduit for heat towards the ice shelf and facilitate the mixing of shelf water masses with ~~MWDW~~MCDW. It is therefore encouraging that eORCA1 (with an effective horizontal resolution under FRIS of 22 km) captures these, as they could play an important role in the evolution of ~~FRIS~~ shelf circulation in future climate scenarios (Naughten et al., 2021).

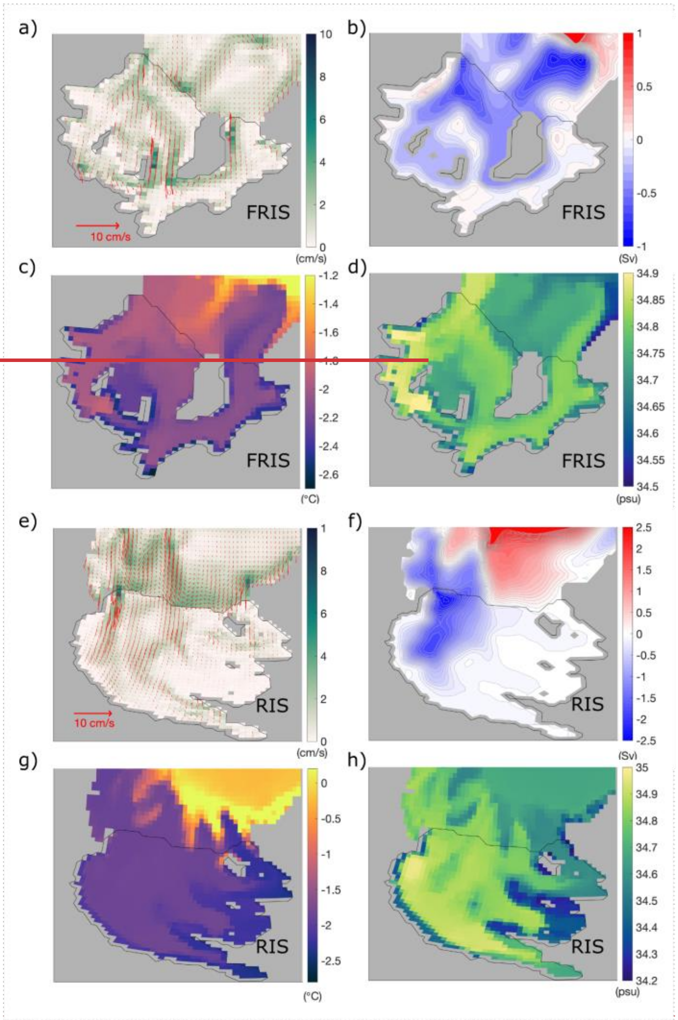

~~Figure 5: Circulation pattern and characteristics of properties under Filchner Ronne (a-d) and Ross (e-h) ice shelves for the last 10 years of the open cavity experiment. Subplots (a) and (e) show depth averaged velocity, (b) and (f) barotropic stream function, (c) and (g) bottom potential temperature and (d) and (h) bottom practical salinity (as opposed to conservative and absolute shown in Bull et al., 2021).~~

### ~~4.2.2 RIS~~

Moving now to the Ross Sea, the time mean circulation pattern under RIS along with the bottom temperature and salinity can be seen in Figs. 5e-5h. Here, we notice a strong anticlockwise circulation concentrated at the western boundary with reduced magnitude currents towards the back and east of the cavity. The west of the cavity is overall warmer and saltier and the east shows signatures of ISW. Bottom temperature indicates the presence of a cold ISW plume exiting the cavity to the far east (Fig. 5g~~)~~), which is not seen in the time averaged velocities or barotropic streamfunction, likely because the associated speeds are ~~extremely~~ slow. Instead, the simulated circulation indicates an offshore advection of sub-ice shelf water following the Challenger Trough (see location marked in Fig. ~~1a~~1b). This water mass is likely recirculated HSSW as its temperature remains at surface freezing point (-1.9 °C). A strong clockwise circulation cell offshore of RIS (red in Fig. 5f) brings warm CDW into contact with the ice shelf front to the east, mixing out the signature of ISW further offshore (Fig. 5g). While this simulated circulation pattern agrees well with that described by observations (Fig. 1; Bergamasco et al., 2003; Budillon et al., 2003), it is likely too strong, resulting in an exaggerated net melt ~~rate~~flux compared to the observational estimates (Table 1; anomalously high melt at the eastern portion of the ice shelf front in Fig. 4c).

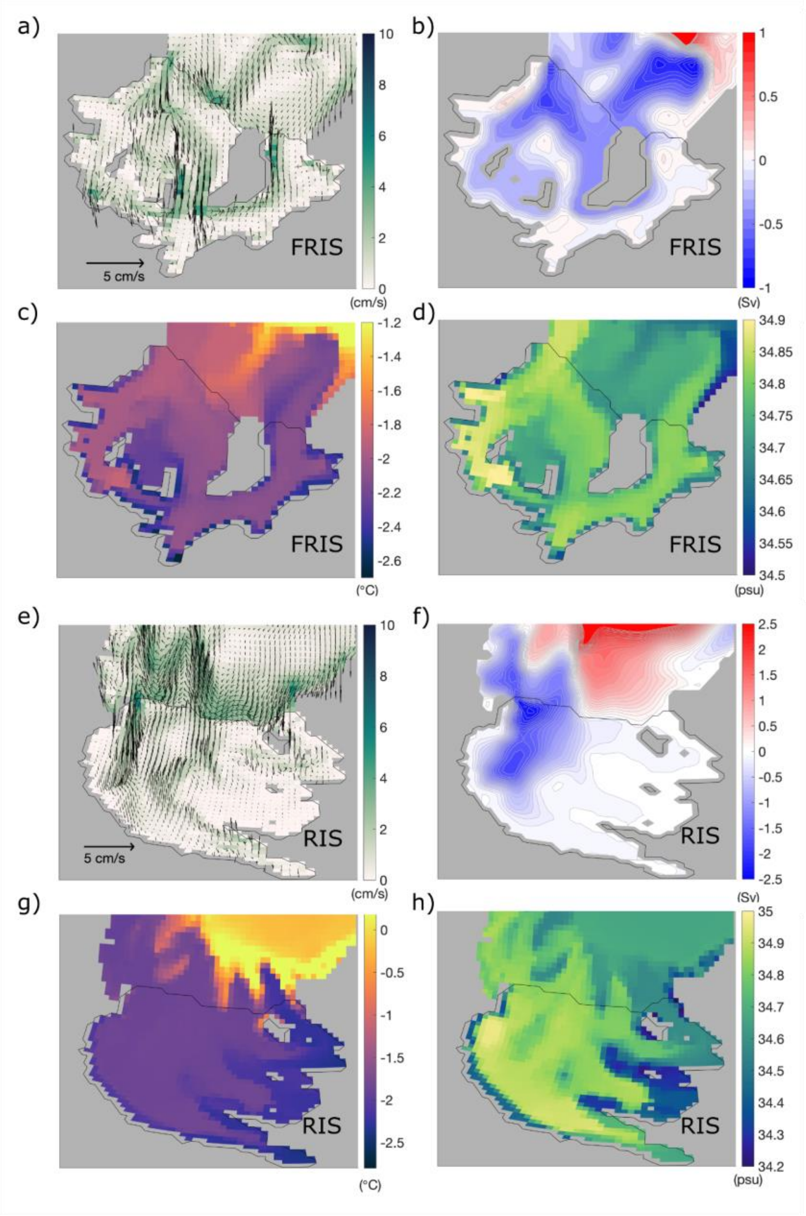
a)
5 cm/s
FRIS
10
8
6
4
2
0
(cm/s)
b)
FRIS
1
0.5
0
-0.5
-1
(Sv)
c)
FRIS
-1.2
-1.4
-1.6
-1.8
-2
-2.2
-2.4
-2.6
(°C)
d)
FRIS
34.9
34.85
34.8
34.75
34.7
34.65
34.6
34.55
34.5
(psu)
e)
5 cm/s
RIS
10
8
6
4
2
0
(cm/s)
f)
RIS
2.5
2
1.5
1
0.5
0
-0.5
-1
-1.5
-2
-2.5
(Sv)
g)
RIS
0
-0.5
-1
-1.5
-2
-2.5
(°C)
h)
RIS
35
34.9
34.8
34.7
34.6
34.5
34.4
34.3
34.2
(psu)

Figure 5: Circulation pattern and characteristics of properties under Filchner Ronne (a-d) and Ross (e-h) ice shelves for the last 10 years of the open cavity experiment. Subplots (a) and (e) show depth averaged velocity, (b) and (f) barotropic stream function, (c) and (g) bottom potential temperature and (d) and (h) bottom practical salinity (as opposed to conservative and absolute shown in Bull et al., 2021).

### 4.3 Impact on offshore properties

To highlight the impact of opening the FRIS, LCIS and RIS sub-ice shelf cavities on the offshore properties, Figs. 2g and 3g show the temperature versus salinity distribution excluding the data under the ice shelves. The differences in bottom temperature and salinity can be seen in Figs. 2h and 2i for the Weddell Sea and 3h and 3i for the Ross Sea.

A significant improvement in the representation of Weddell shelf water properties is evident as now HSSW is within the observed range and ISW is detected on the continental shelf (see HSSW and ISW red boxes in Fig. 2g). Opening the sub-ice-shelf cavity of FRIS has allowed the HSSW that previously built up in the Ronne Depression to advect under the ice shelf, become modified through basal interactions and exit the cavity as colder and fresher ISW. Consequently, the temperature and salinity differences are polarized west and east with warmer fresher conditions along the entire western boundary of the Weddell Gyre and cooler saltier conditions on the eastern continental shelf (Figs. 2h and 2i). These results agree well with those of Mathiot et al. (2017). The impact of opening LCIS can be seen via the maintenance of cold bottom properties immediately to the north (despite the fact that the shelf circulation has changed so that HSSW no-longer floods this region), along with the presence of a large negative salinity anomaly indicative of ice shelf melt (Fig. 2i). As the simulation is only 124 years long, the impact of opening the cavities on AABW cannot be fully assessed due to the slow renewal of this water mass at the bottom of the global ocean. A small change in signature of AABW can, however, be seen in the volumetric T-S plot (~~supplementary material~~Supplementary Material Fig. ~~S1a)~~S3a), where explicit ocean-ice shelf interaction results in a shift in volume towards cooler, fresher~~, slightly cooler~~ AABW~~.~~ (Open - Closed weighted average shift in AABW volume by -0.008 °C and -0.003 psu). This shift is accompanied by a small increase in volume of the water mass by 0.23 % (AABW limits delineated in green in Fig. ~~S1a~~S3a).

The impact of opening the RIS cavity on offshore properties can be seen in Figs. 3h and 3i. Similar to the Weddell Sea, conditions in the west, where in the reference run HSSW was built up, now become warmer and fresher as the path under the ice shelf is open. The signature of the cold plumes of dense shelf water (Fig. 5g) on either side of Roosevelt Island can clearly be seen in the temperature difference plot (Fig. 3h), but curiously they do not possess the same salinity anomaly (Fig. 3i). The positive salinity difference of the western plume indicates that this water is a variety of HSSW which has circulated under the ice shelf and was previously not present in this area. The small negative anomaly to the east indicates that this cold plume is, as previously ~~hypothesized~~hypothesised, outflowing ISW. Small temperature differences on the continental slope and further offshore indicate that there has been some communication of the changes in shelf waters further afield. The volumetric T-S plot for the Ross Sea found in ~~supplementary material~~Supplementary Material (Fig. ~~S1b~~S3b) indicates that opening the RIS cavity has moved the core of AABW towards slightly cooler fresher values, accompanied by a 0.34 % decrease in volume of AABW as defined by the original water mass limits (delineated in green in Fig. ~~S1b).~~S3b; Open - Closed weighted average shift in AABW volume by -0.001 °C and -0.005 psu).

### 4.4 Comparison with ice shelf front CTD observations

The differences in circulation patterns and in thermohaline properties that result from opening the RIS and FRIS cavities documented above do not elucidate whether or not we have reduced biases and improved the realism of shelf waters in eORCA1. For this, a direct comparison with in-situ observations is necessary. Due to the remote location of these ice shelves and the harsh conditions associated with obtaining hydrographic samples in these areas, there are limited observations, and so optimally interpolated atlases such as WOA or ocean reanalysis products like SOSE miss important local features or seasonal variability. For comparison purposes, we have consequently selected CTD data from research cruises that have sampled transects across the front of the ice shelves and extracted the model data corresponding to the approximate ship's track using PAGO, a ~~pre-existing~~ tool to analyze gridded ocean datasets (Deshayes et al., 2014).

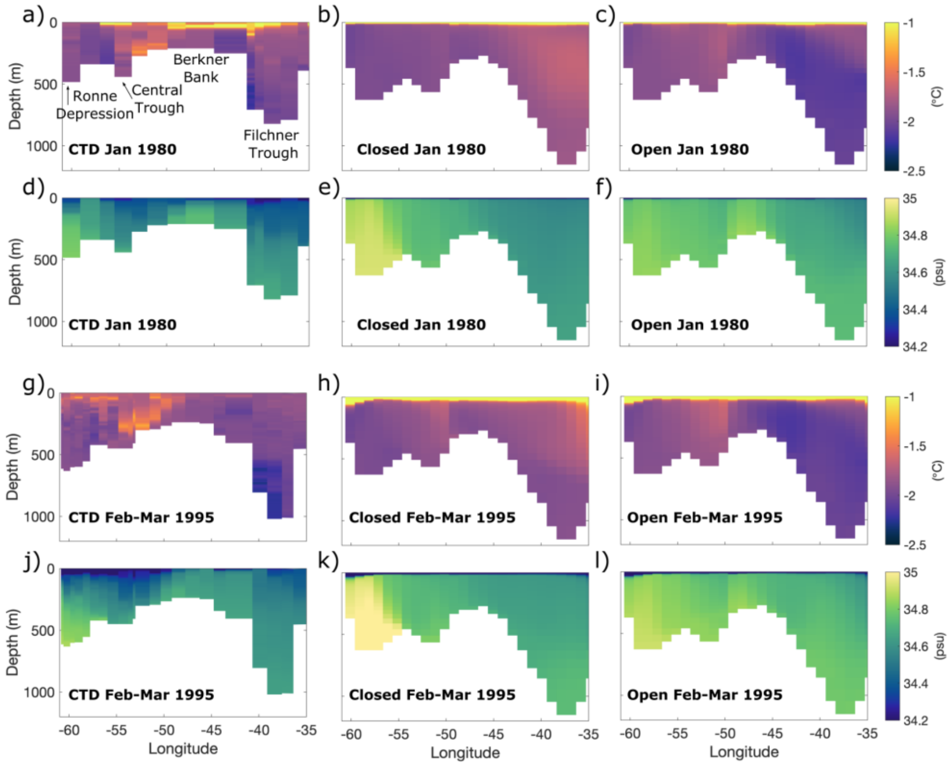

Figure 6: Validation of properties across the Filchner Ronne Ice Shelf front by comparing closed and open cavity NEMO results with measured values from CTD sections performed in 1980 (Rohardt et al., 2016) and 1995 (Janout et al., 2021).

The model output for the corresponding equivalent year and month was extracted for more accurate comparison. Bathymetric features discussed in the text are labelled in subplot (a).

For FRIS we use two CTD sections across the ice shelf front undertaken in 1980 and 1995 on board the RV Polarstern by the Alfred Wegener Institute (Rohardt et al., 2016; Janout et al., 2021). The location of the section selected in NEMO to approximately overlay the CTD transects can be seen as a magenta dotted line in Fig. ~~For FRIS we use two CTD sections across the ice shelf front undertaken in 1980 and 1995 on board the RV Polarstern by the Alfred Wegener Institute (Rohardt et al., 2016; Janout et al., 2021). The location of the section selected in NEMO to approximately overlay the CTD transects can be seen as a magenta dotted line in Fig. 1b~~1a. The output from NEMO corresponding to the same months and same equivalent year (for the second cycle of CORE forcing) in the simulation was selected for both “Closed” (prescribed freshwater flux) and “Open” (FRIS, LCIS and RIS) cavity runs. A comparison between the CTD data and NEMO can be seen in Figs. 6a to 6f for January 1980 and Fig. 6g to 6l for February to March 1995. In terms of surface waters, NEMO does not capture the fine scale horizontal variability and overestimates the subsurface salinity. For both observational years, evidence of warm, fresh, MCDW intrusions can be seen in the middle of the CTD sections (Central Trough; Figs. 6a and 6g). While the model struggles to capture the coherence of this sub-surface temperature maximum, the counterclockwise circulation cell ~~setup~~set up on the central continental shelf in the open cavity simulation does aid the advection of MCDW towards the ice shelf, thereby producing a slightly better representation of this warm intrusion in Figs. 6c and 6i. The presence of cold ISW in Filchner Trough is clearer in the 1995 CTD data than in 1980 where the sampling frequency was sparser and this region not well covered. The 2018 Polarstern sampling of the Jason Trough was the highest resolution yet and while we cannot directly compare with the simulation output as the CORE forcing ends in 2009, ~~evidence for~~ the presence of a tongue of ISW focused on the western bank of Filchner Trough is evident in Fig. 3 of Janout et al. (2021) and so should be kept in mind for comparison. Opening the FRIS cavity overall improves the thermohaline properties at the ice shelf front, most notably by spreading out the pool of HSSW from the ~~Berkner~~Ronne Depression (e.g. Fig. 6k) across the continental shelf (e.g. Fig. 6l) and by facilitating the production and thus outflow of ISW within Filchner Trough (Figs. 6c and 6i).

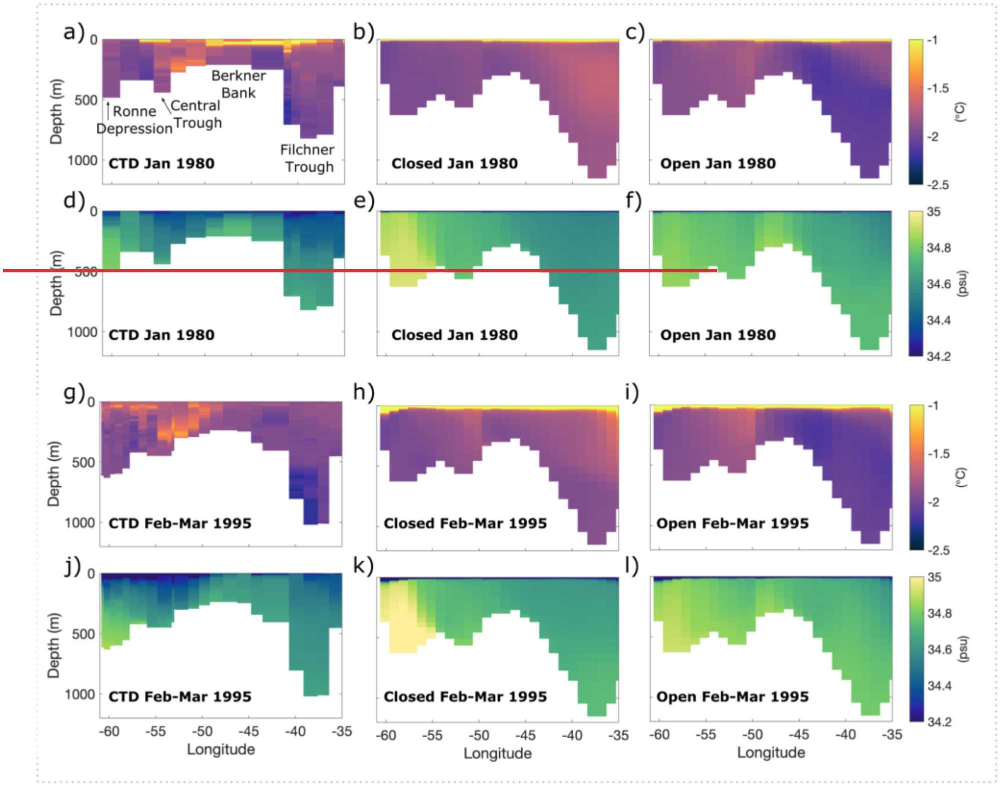

~~Figure 6: Validation of properties across the Filchner Ronne Ice Shelf front by comparing closed and open cavity NEMO results with measured values from CTD sections performed in 1980 (Rohardt et al., 2016) and 1995 (Janout et al., 2021). The model output for the corresponding equivalent year and month was extracted for more accurate comparison. Bathymetric features discussed in the text are labelled in subplot (a).~~

The CTD sections used for comparison along the front of RIS were obtained through the World Ocean Circulation Experiment Database (Boyer et al., 2018) and correspond to cruises undertaken on board the RVIB Nathaniel B. Palmer in 2000 (cruise id: US010404; Smethie and Jacobs, 2005) and in 2007 (cruise id: US034357). Data was extracted from the eORCA1 simulation corresponding to the dates of these cruises and the approximate ship track across the ice shelf front (magenta dotted line in Fig. ~~1a~~1b). Similar to the Weddell Sea, the model tends to overestimate the subsurface temperature and salinity (Figs. 7b, 7e, 7h and 7k), suggestive of biases in the representation of coastal processes, including vertical mixing. This effect is somewhat reduced by allowing for circulation under RIS, especially by decreasing subsurface salinities

(~~Figues~~Figures 7f and 7l). At depth, NEMO captures the east-west distribution of haline properties such as the HSSW pool located within Joides Basin, albeit with somewhat amplified salinities. In terms of temperature, the model has a clear bias to the east, especially in the closed cavity run, where CDW is detected at the ice shelf front. Both the temperature and salinity biases are reduced in the open cavity run (e.g. Figs. 7c and 7f). In particular, the significant reduction in the extent and magnitude of the sub-surface warm water intrusions brings the model more in-line with observations.

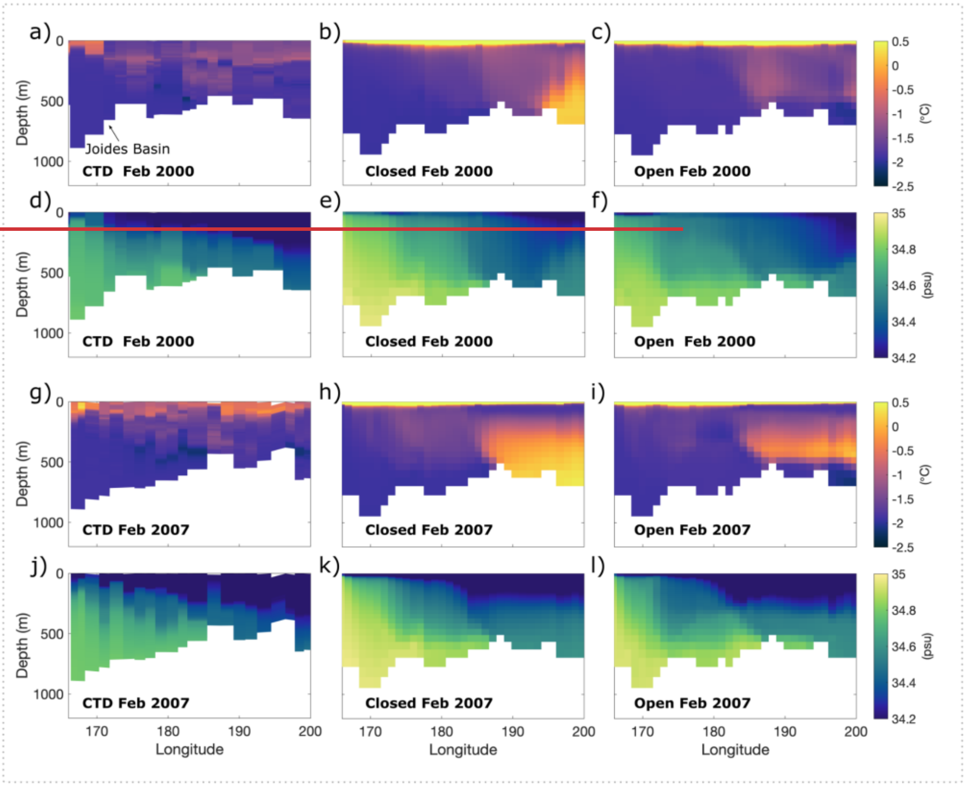

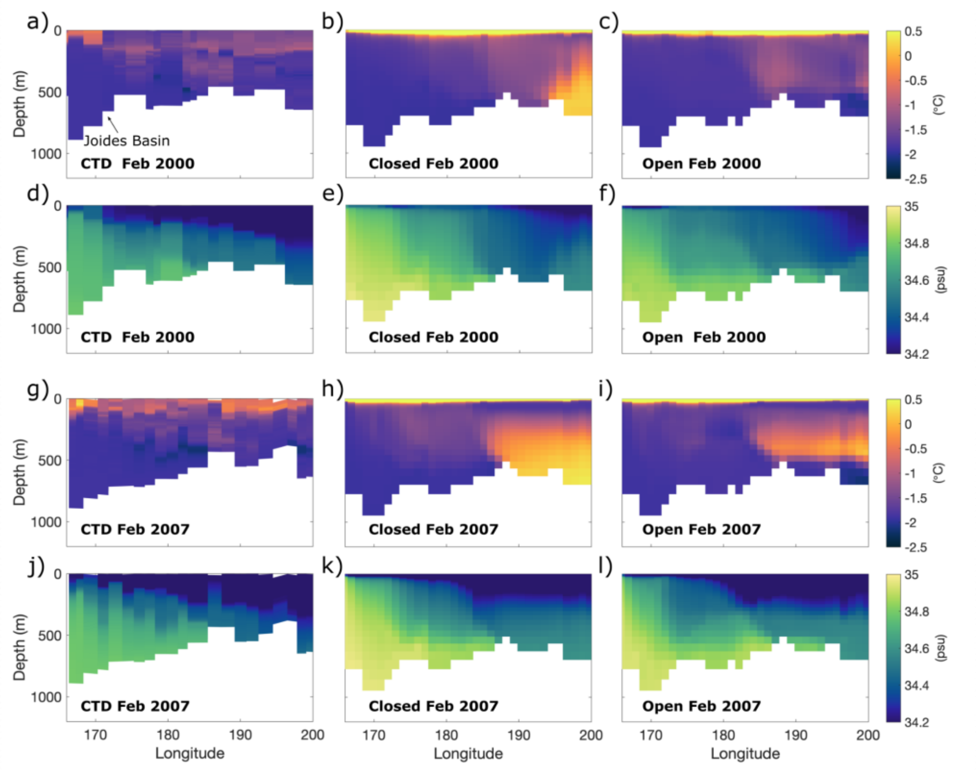

Figure 7: Same as Fig. 7 but for Ross Ice Shelf front for CTD sections performed in 2000 (Smethie and Jacobs, 2005) and 2007 (Boyer et al., 2018).

A recurring theme throughout the results presented here is that the model is overall too salty, driven by what appears to be an over-production of HSSW in the Ronne Depression and Joides Basin. One driver for this could be the ~~hyper-~~overestimated polynya activity ~~of dense water formation via open-ocean convection~~ which forms the totality of parent waters of AABW in the absence of ice shelves in eORCA1. This can be seen in ~~Supplementary Material~~ Fig. ~~S2~~8 where the mean winter (July-August-September) mixed layer depths (MLD) in the reference run for the years 1971-2009 ~~(Fig. S2c and S2d)~~ are compared to the climatology from Sallee et al. (2021) for the same time period and using the same criteria for calculation (Fig. ~~S2a~~8a and ~~S2b~~8b; MLD defined as the depth at which density exceeds the 10 m density by 0.03 kg $m^{-3}$). The model greatly overestimates winter MLDs in the Weddell Sea, both on the continental shelf adjacent to FRIS, where the depth of the base of the mixed layer aligns with bathymetric features indicating deep convection right to the ocean floor, and offshore of the continental slope where a large region of MLD greater than 1000m is present (Fig. ~~S2c~~8c). This level of open ocean deep convection has in reality only once been observed, during the 1974-1976 Weddell Polynya~~,~~ event near Maud Rise (3º E, 66º S), indicating a gross overestimation of winter MLDs in the model (Heuze et al., 2021; Killworth et al., 1983). Ross Sea MLDs (Fig. ~~S2d~~8d) compare better with observations, but show values indicating a full water-column-depth convection in Terra Nova Bay which is not reported in Sallee at al. (2021). Curiously, NEMO actually under-estimates winter mixed layers in the eastern portion of the Ross continental shelf showing mean MLDs of under 100m where the observational climatology indicates values of around 400m (Fig. ~~S2d~~8d compared to Fig. ~~S2b~~8b). This too-strong stratification could be one of the factors facilitating the intrusion of CDW to the ice shelf front seen in Figs. 7b and 7h.

~~Note that if ISW is explicitly formed, as in the open cavity experiment, the exaggerated deep convection on the shelf should be reduced, otherwise the signatures of ISW and modified HSSW will simply be mixed out. Some reduction in MLD is seen on the continental shelf and slope in the Filchner (Fig. S2e) and Challenger Troughs (Fig. S2f) due to the increase in stratification as a result of the greater bottom densities present in these areas (Fig. S5a and S5c) and surface freshening (Figs. 8d and 9d). Conversely, the regions of exaggerated MLDs, offshore in the center of the gyre of the Weddell Sea, and in Terra Nova Bay in the Ross Sea actually deepen (positive anomalies Figs. S2e and S2f). This highlights the need for work to be done on reducing wintertime deep convection and would complement efforts underway on better representing dense water overflows.~~

The authors note that the ~~biassed~~biased MLDs could be one of a number of factors ~~driving~~contributing to the overly saline conditions; wrong sea-ice parameters and biases in the atmospheric forcing could also play an important (and related) role. High sea ice production is seen on the southwest continental shelves of the Weddell and Ross Seas in Supplementary Figs. ~~S3c~~S2a and ~~S4c~~S2b. Opening the cavities slightly reduces the magnitude of ice production in the Ronne Depression (Fig. ~~S3d~~S2c) and at the location of the Terra Nova Bay Polynya (Fig. ~~S4d) but~~S2d) and increases the production of ice ~~(and thus HSSW)~~ further east. ~~The result~~There is ~~a re-organisation of~~ no overall change in the ~~locations~~principal location of polynya activity and the slight west/east decrease/increase in sea ice is presumed to have a negligible effect on the total amount of HSSW ~~formation and a redistribution~~generated. As such, the reduction of the ~~continental shelf circulation. This does~~ highly saline HSSW signature seen in Figs. 2g and 3g when cavities are opened is likely due to a conversion to ISW (and not ~~fully correct for the net over~~ from a decrease in HSSW production ~~of HSSW and thus the positive salt bias seen in Figs. 6 and 7, but it does work towards decreasing bottom salinities offshore (Figs. 2i and 3i) and bringing the HSSW signature more in line with observations (Figs. 2g and 3g).~~itself). Please see the Supplementary Information Sect. 3 for an ~~in-depth~~ evaluation of simulated ~~sea ice~~polynyas near the studied ice shelves and a diagnosis ~~on~~of the effect of opening the cavities on ~~sea~~ ice production.

Once a model is able to explicitly form the parent waters of AABW in the right locations on the continental shelf (and export this dense water), it will become necessary for modelers to tone-down open ocean deep convection as this workaround will be longer relied upon to form the totality of AABW. Here we explore the impact that opening the cavities has on MLD to diagnose the extent of vertical convection in the model. Some reduction in MLD is seen on the continental shelf and slope in the Filchner (Fig. 8e) and Challenger Troughs (Fig. 8f) due to the increase in stratification as a result of the greater bottom densities associated with outflowing ISW (Fig. S4a and S4c). The presence of ISW appears to promote slightly increased ice production in these areas, as discussed earlier. In this case, it is therefore the ocean properties that drive sea ice and the brine rejection associated with elevated ice production is found to have a minor effect on water properties. Within the region of exaggerated MLDs off the Weddell continental slope, the MLDs deepen in the “Open” cavity experiment (positive anomalies Figs. 8e). We hypothesise that this deepening is associated with an overall cooling of the subsurface layers due to a horizontal mixing of ISW, unimpeded by a relatively weak and diffuse Antarctic Slope Current (discussed in the following section). Overall, in wintertime, mixed layers are on average 19 m deeper over the whole Weddell Sea region in the “Open” cavity experiment compared to the reference “Closed” simulation. This reinforcement of the high MLD bias highlights the need for work to be done on reducing wintertime deep convection, together with better representing dense water overflows.

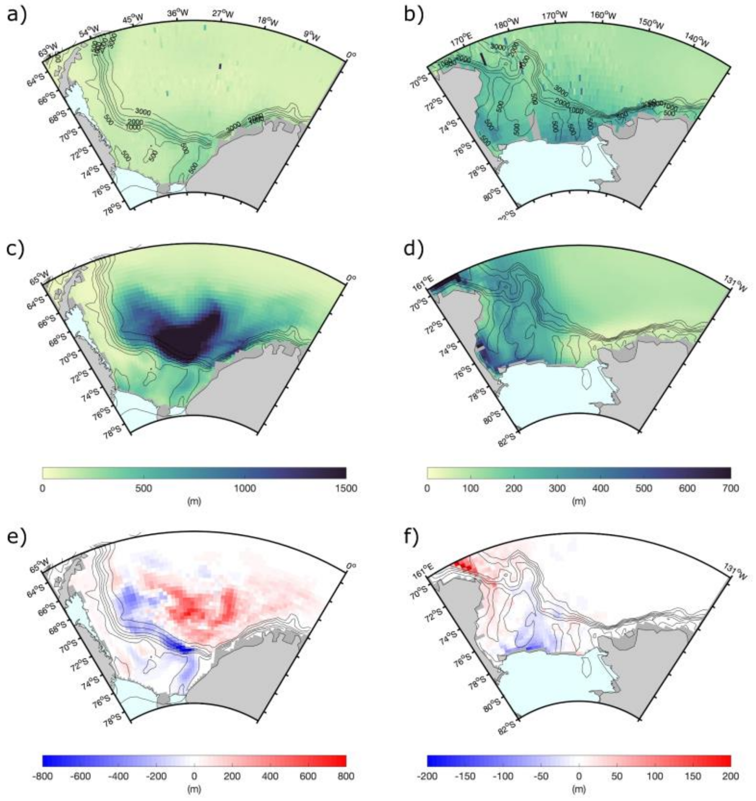

Figure 8: Winter mixed layer depths (MLD) from observational atlas of Sallee et al. (2021) shown in (a) and (b) for the Weddell and Ross Sea respectively, are compared with the winter mean from NEMO v4.2 eORCA1 forced model reference configuration equivalent years 1971-2009 in (c) and (d). The differences in MLDs between the “Open” cavity run and reference “Closed” run are shown in subplots (e) and (f).

### 4.5 Offshore export of continental shelf properties

We have seen how opening the large, cold, ice shelf cavities in eORCA1 leads to a better representation of continental shelf circulation and thermohaline property distributions. But the question remains regarding the transfer of these now more realistic dense shelf waters~~,~~ downslope and offshore, to feed the globally important AABW. While the simulation period of 124 years (~~2~~two CORE forcing cycles) is too~~-~~ short to explore the impact of these changes far~~-~~ afield, it is sufficient to investigate the changes on the continental shelf and slope adjacent to the large ice shelves. To do this, we use PAGO (Deshayes et al., 2014) to select a cross section of data following the bathymetric troughs of the Weddell and Ross Seas which are thought to be important for dense water export~~,~~ (Foldvok et al., 1985; Jacobs, 1991), namely the Filchner and Challenger Troughs (sections shown in green in Fig. 1).

~~The thermohaline and velocity cross sections of Filchner Trough and a continuation down the continental slope can be seen in Figs. 8a and 8b for the open cavity run and the difference between these values and the reference run (Open-Closed) are shown in Figs. 8c and 8d. By opening the sub-ice shelf cavity, the properties within Filchner Trough have decreased in temperature and increased in salinity as the candidate-parent waters of AABW build up on the continental shelf. This results in a net increase in density at the bottom of the trough (Fig. S5b), but there is very little indication of a coherent cascading of this water down the continental slope.~~

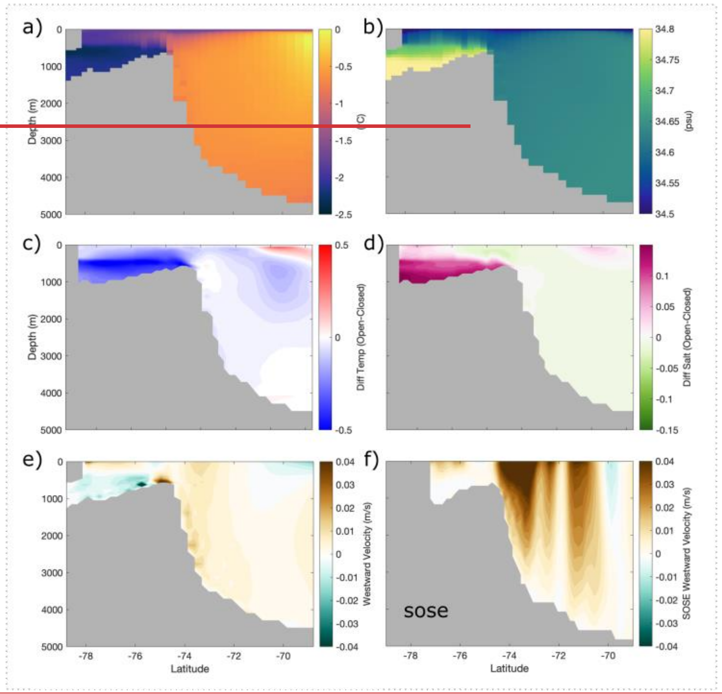

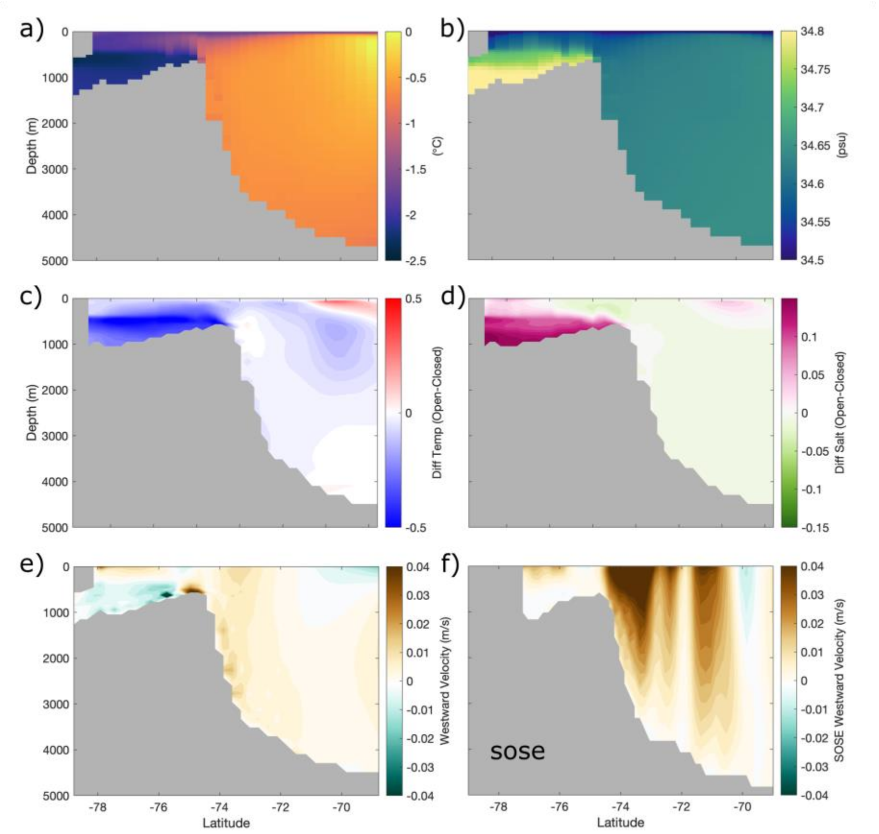

Figure ~~8~~9: Cross section of properties along the Filchner Trough and down the adjacent continental slope of the Weddell Sea for (a)-(e) NEMO and (f) SOSE. Subplots (a) and (b) show temperature and salinity for the open cavity configuration, to be compared to (c) and (d) which show the differences (Open - Closed) with the reference configuration. Subplot (e) shows cross sectional velocities with westward as positive for the open cavity run, to be compared with SOSE values shown in subplot (f).

The thermohaline cross sections of Filchner Trough and a continuation down the continental slope can be seen in Figs. 9a and 9b for the open cavity run and the difference between these values and the reference run (Open-Closed) are shown in Figs. 9c and 9d. By opening the sub-ice shelf cavity, the properties within Filchner Trough have decreased in temperature and increased in salinity as the candidate parent waters of AABW build up on the continental shelf. This results in a net increase in density at the bottom of the trough (Fig. S4b), but there is very little indication of a coherent cascading of this water down the continental slope.

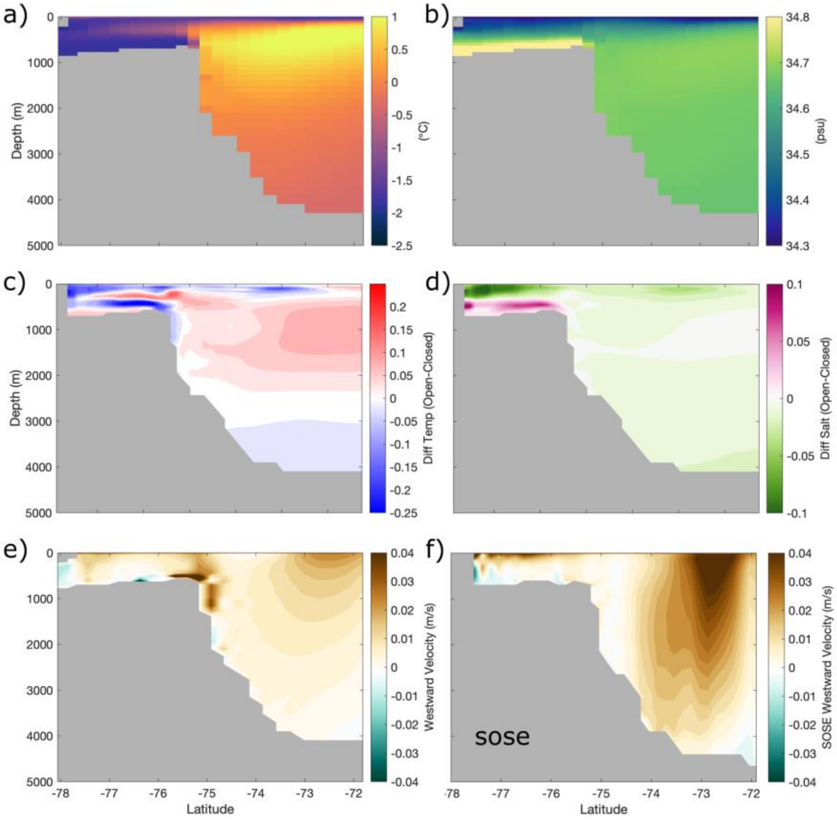

Figure 10: Same as Fig. 9 but for the Challenger Trough and the Ross Sea continental slope.

A cross section of the Challenger Trough (Fig. ~~9),~~10) reveals depth-varying thermohaline changes~~ as opening~~. Opening the sub-ice shelf cavity has allowed for the water adjacent to the ice shelf to advect into the cavity leaving the bottom properties here slightly warmer~~, while the~~. The layer immediately above conversely experiences cooling and salinification due to the outflow of ISW driven by the 'ice pump' (Fig. ~~9c~~10c). Here we see some evidence indicating the translation of this dense cold water tongue over the continental shelf break and downslope (Figs. ~~9c~~10c and ~~S5d~~S4d). The overflow of this water results in the pulling in of warmer offshore water at intermediate depth (Fig. ~~9c~~10c).  A horizontal redistribution of surface waters simultaneously takes place due to the anti-clockwise circulation pattern (Fig. 5e) which in turn produces a cooling and freshening in the surface layer (Figs. ~~9c~~10c and ~~9d~~10d).

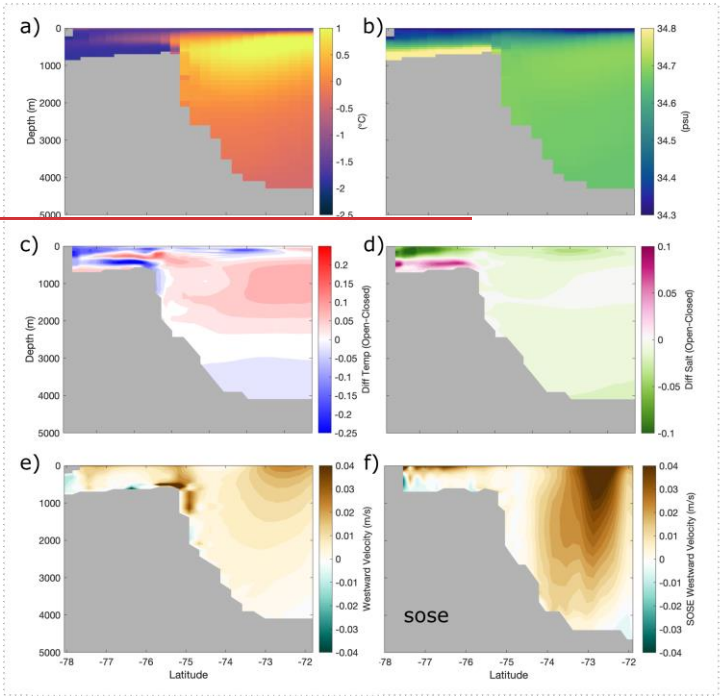

~~Figure 9: Same as Fig. 9 but for the Challenger Trough and the Ross Sea continental slope.~~

For both the Filchner and Challenger Troughs, the downslope export of the ISW tongue is limited due to the commonly-known and acknowledged problem of correctly capturing this overflow in a coarse z-coordinate model (Heuze et al., 2021). The aptitude of representing dense water overflows is thought to increase with models of higher resolution, but this is difficult to achieve in a global model for climate coupling purposes without a nested zoom (Storkey et al., 2018; Colombo et al., 2020; Solodoch et al., 2022).

Another important dynamic for Antarctic shelf water realism is the ~~Antarctic Slope Current (~~ASC~~;~~ (red arrows in Fig. 1) and related Antarctic Slope Front, which together restrict the lateral mixing of offshore and shelf water masses, acting as an effective barrier protecting the large cold ice shelves from warm water masses of circumpolar origin (Thompson et al., 2018). Some CDW, or a modified version thereof, is carried within the ASC and occasionally fluxes onshore to mix with dense shelf waters (Beadling et al., 2020; Bull et al., 2021). This interaction between dense shelf water and CDW is important for the formation of AABW, as the onshore flux of water replaces the dense water transported offshore and thus sustains formation of shelf water (Thompson et al., 2018). Figure ~~8e~~9e shows a velocity cross section for the Weddell Sea shelf and slope where westward velocities are positive so as to correspond with the direction of the ASC and the net westward transport across the section is 9.~~8Sv.~~8 Sv (1 Sv is $10^6$ $m^3$ $s^{-1}$). This can be compared to Fig. ~~8f~~9f which is a cross section from SOSE output (same time periods used) where the net transport is three times higher at 32.~~8Sv~~8 Sv. Similarly for the Ross Sea, Fig. ~~9e~~10e shows a cross section of westward velocities in eORCA1 where the volume transport is 13.~~3Sv~~3 Sv which is less than half of that estimated from SOSE in Fig. ~~9f~~10f of 20.~~9Sv~~9 Sv. As can be seen from both SOSE cross sections, the ASC flows eastward as a narrow jet, closely following the shelf break in the Weddell Sea and slightly further offshore in the Ross Sea. It is well known that coarse resolution models are unable to correctly represent the ASC as a resolution of at least 0.5° is needed to capture the dynamics and net transport (Mathiot et al., 2011). The absence of realistic ASC in NEMO eORCA1 (Figs. ~~8e~~9e and ~~9e~~10e) has important consequences, as a weaker and more diffuse ASC allows for ~~the~~a greater level of onshore-offshore exchange of water masses~~ and~~. This is ~~a~~one important restriction that needs to be kept in mind when using this coarse resolution configuration for process studies in the area.

## 5 Summary and Discussion

Explicitly representing ocean-ice shelf interactions is of great interest to modelers as these processes play an important role in global ocean dynamics, climate and future sea level rise. The formation of dense shelf waters (HSSW and ISW) along the Antarctic coastline provides the principal source for AABW, which in turn facilitates the ventilation of the deep ocean and constitutes the lower limb of the global overturning circulation (Killworth, 1983; Johnson, 2008; Orsi, 2010).

Our results focus on the Weddell and Ross seas as they are respectively the main ventilation source of the abyssal Atlantic and Indian basins, and the abyssal Pacific basin (Solodoch et al., 2022). Explicitly simulating the sub-ice shelf cavities of FRIS and LCIS in the Weddell Sea leads to a re-organisation of continental shelf circulation with thermohaline patterns in agreement with those reported by other NEMO model studies (Mathiot et al., 2017; Storkey et al., 2018 and Bull et al., 2021), namely warming and freshening in the west and cooling and salinification in the east. Notably, opening a pathway for HSSW under FRIS allows for an anticlockwise circulation of water under the ice shelf, triggering basal melt and re-freezing, and producing the super-cold ISW. ~~In both the Weddell and Ross Seas, opening the cavities decreases sea ice production to the west of the ice shelves, assisting in the partial reduction of the salt bias in these areas linked to polynya activity.~~

By comparing model output with two CTD sections performed across the front of FRIS in 1980 and 1995 (Rohardt et al., 2016; Janout et al., 2021), we see clear evidence of an improvement in the realism of water properties with the opening of the sub-ice shelf cavity. Similarly in the Ross Sea, an anticlockwise sub-ice shelf cavity circulation cell facilitates the spread of HSSW across the continental shelf and ocean-ice shelf interactions create a cold ISW plume to the east of Roosevelt Island. By evaluating the model output against CTD sections performed in 2000 and 2007 (Smethie and Jacobs, 2005; Boyer et al., 2018), we see that opening the cavity significantly ameliorates the sub-surface warm water bias otherwise seen to the east of RIS in the reference configuration, and brings a significant improvement in the horizontal thermohaline distributions.

The ~~net~~mean total melt ~~rates~~fluxes of FRIS, LCIS and RIS are found to be within the uncertainty range of observational estimates and other model studies. Notably, the melt rate pattern of FRIS agrees surprisingly well with the high resolution regional model of Haussmann et al. (2020) and the satellite observations of Rignot et al. (2013), showing details of melt and refreezing that were not expected at a 1° resolution, although the meanders of the grounding line are not well represented at 1°. For RIS, the net melt is higher than all observed estimates but lower than that predicted by other model studies. RIS melt rates are strongly related to the supply of warm water to the ice shelf base (Arzeno et al., 2014), and correctly representing this in models presents a challenge due to the close proximity of CDW to the ice shelf front in this area.

Meltwater and modified HSSW mix on the continental shelves of the Weddell and Ross Sea and in reality cascade down the continental slope, mixing with ambient water masses during the descent, to eventually feed AABW. This process is poorly represented in NEMO eORCA1, a common problem with coarse z-coordinate models, as exaggerated vertical and horizontal mixing erodes the signatures of the dense overflow tongue. As mentioned by Storkey et al. (2018), the use of a terrain following coordinate system (known as sigma coordinate) can greatly improve the representation of these density currents, and so is something worth exploring in the future. Improvement in the representation of the overflows along with a reduction of open-ocean deep convection should together allow for a coherent communication of the now more realistic properties of dense water on the continental shelf offshore to AABW.

## 6 Conclusion

In this paper the authors focus on improving the properties of AABW parent waters in a global NEMO configuration. We compare the model simulations with~~ local~~ in situ observations, in addition to gridded climatologies, so as to deepen understanding and expertise regarding the impact of opening sub-ice shelf cavities on ocean dynamics. As ocean models used for climate simulations with multiple scenarios (such as CMIP) need to be at a coarse resolution to permit long integrations, we use the NEMO global ocean 1° configuration, eORCA1, here. The results presented are for CORE inter-annual forcing, with a fixed cavity geometry, as this allows us to clearly identify the impact of ocean-ice shelf interactions at a few critical locations without the obscuring effect of coupling feedbacks. We present here a validated configuration of NEMO 4.2 eORCA1 with explicit ocean-ice shelf interactions only within the largest 3 cold~~-core~~ cavities: FRIS, LCIS and RIS. Limitations of this choice are that together FRIS, LCIS and RIS only represent 63 % of the total area of Antarctic ice shelves and, while they are responsible for the formation of the majority of the parent waters of AABW, interactions with remote unresolved ice shelves ~~is~~are missing (Nakayama et al., 2020). The next steps in terms of increasing complexity in NEMO eORCA1 are to open other intermediate size cavities, such as Amery, Riiser-Larsen and Fimbul, in a fixed geometry configuration~~.~~, and leave smaller cavities parameterized due to resolution constraints. As the residence time needed to flush these ~~smaller~~intermediate cavities is shorter than for FRIS and RIS, we suggest that the complex initialization methods presented here are not needed. This work is aimed at building understanding so as to eventually move to coupling with an ice sheet model thereby allowing for fully evolving cavity geometry and iceberg calving from the ice shelf front.

Given the critical role that the Southern Ocean plays in regulating global climate, it is paramount that ocean models work towards improving the representation of key processes in order to provide state-of-the-art simulations of the ocean in a changing climate (Beadling et al., 2020). The global configuration of NEMO presented here, has been proven to improve the realism of water masses in the Weddell and Ross Seas. We advocate for climate modelers to use it, as it enables a more accurate representation of the formation of the parent waters of AABW, and a first step in the perspective of representing ocean-ice shelf interactions in climate applications.

## 7 Author contribution

KH, JD and PM together contributed to the conceptualization of the research outlined in this manuscript. KH led the formal analysis and investigation with the assistance of JD, CR, CL, NJ and PM. MV led the sea ice research component with assistance from CR and CL. Validation of the model was undertaken by KH with PM. CE led the programming, code management and supervised all the model runs undertaken by KH. The project was supervised by JD and NJ, providing guidance and critical feedback. The whole group contributed to the writing and review of the submitted manuscript.

## 8 Competing interests

The authors declare that they have no conflict of interest.

## 9 Acknowledgements of financial support

Katherine Hutchinson received financial support of the European Union’s Horizon 2020 research and innovation programme Marie Skłodowska-Curie grant agreement No 898058 (Project OPEN). Nicolas Jourdain received support from the European Union’s Horizon 2020 research and innovation programme under grant agreement no. 101003536 (ESM2025). Pierre Mathiot acknowledges support from the European Union’s Horizon 2020 research and innovation programme under grant agreement no. 820575 (TiPACCs). This work was performed using HPC resources from GENCI–IDRIS (Grant 2021-A0100107451) and from the IPSL Mesocentre ESPRI.

## 10 Code and data availability

The NEMO ocean model code is available via open software license from the NEMO website (https://www.nemo-ocean.eu). The NEMO output for the Weddell and Ross Seas (focus of this study), plus the namelists used, bathymetry, ice shelf draft, freshwater input and initial condition files are available via the data repository stored here: https://doi.org/10.5281/zenodo.7561767. Some example scripts for data extraction, calculations and plotting can also be found in this repository. The World Ocean Atlas hydrographic data of Locarnini et al. (2019) and Zweng et al. (~~2018~~2019) can be found here: https://www.nodc.noaa.gov/OC5/woa18/woa18data.html and Southern Ocean State Estimate data of Mazloff et al. (2010) can be accessed here: http://sose.ucsd.edu/sose_stateestimation_data_05to10.html. The mixed layer depth data from Sallee et al. (2021) can be accessed here: https://doi.org/10.5281/zenodo.5776180. The CTD transects used for comparisons across the ice shelf front for FRIS 1980 and 1995 can be respectively found here: https://doi.org/10.1594/PANGAEA.860066 and here https://folk.uib.no/ngfso/Data/CTD/. The RIS CTD data from the 2000 (US010402) and 2007 (US034357) RVIB Nathaniel B. Palmer cruises are available from the World Ocean Data Base at https://www.nodc.noaa.gov/OC5/WOD/pr_wod.html. The PAGO toolbox used to extract model output along a line in front of the ice shelf from Deshayes et al. (2014) can be accessed here: https://www.whoi.edu/science/PO/pago/.

## References

~~Abrahamsen, E. P., Meijers, A. J., Polzin, K. L., Naveira Garabato, A. C., King, B. A., Firing, Y. L., Sallée, J., Sheen, K. L., Gordon, A. L. and Huber, B. A.: Stabilization of dense Antarctic water supply to the Atlantic Ocean overturning circulation, Nature Publishing Group, 2019.~~

~~Adusumilli, S., Fricker, H. A., Medley, B., Padman, L. and Siegfried, M. R.: Interannual variations in meltwater input to the Southern Ocean from Antarctic ice shelves, Nature Publishing Group, 2020.~~

Arndt, J. E., Schenke, H. W., Jakobsson, M., Nitsche, F. O., Buys, G., Goleby, B., Rebesco, M., Bohoyo, F., Hong, J. and Black, J.: The International Bathymetric Chart of the Southern Ocean (IBCSO) Version 1.0—A new bathymetric compilation covering circum-Antarctic waters, ~~Wiley Online Library~~Geophys.Res.Lett. 12, 2013.

Asay-Davis, X. S., Cornford, S. L., Durand, G., Galton-Fenzi, B. K., Gladstone, R. M., Gudmundsson, G. H., Hattermann, T., Holland, D. M., Holland, D. and Holland, P. R.: Experimental design for three interrelated marine ice sheet and ocean model intercomparison projects: MISMIP v. 3 (MISMIP ), ISOMIP v. 2 (ISOMIP ) and MISOMIP v. 1 (MISOMIP1), ~~Copernicus GmbH~~Geoscientific Model Development 7, 2016.

Beadling, R. L. L., Russell, J. L., Stouffer, R., Mazloff, M. R., Talley, L. D., Goodman, P. J., Sallee, J. B., Hewitt, H., Hyder, P. and Pandde, A.: Simulation of Southern Ocean Properties Across Model Generations and Future Changes under Continued 21 st Century Warming in CMIP6. 2020.

Bergamasco, A., Defendi, V., Zambianchi, E. and Spezie, G.: Evidence of dense water overflow on the Ross Sea shelf-break, ~~Cambridge University Press~~Antarct.Sci. 3, 2002.

Bergamasco, A., Defendi, V., Del Negro, P. and Umani, S. F.: Effects of the physical properties of water masses on microbial activity during an Ice Shelf Water overflow in the central Ross Sea, ~~Cambridge University Press~~Antarct.Sci. 3, 2003.

Bitz, C. M., Holland, M. M., Weaver, A. J. and Eby, M.: Simulating the ice-thickness distribution in a coupled climate model, ~~Wiley Online Library~~Journal of Geophysical Research: Oceans C2, 2001.

Bowen, M. M., Fernandez, D., Forcen-Vazquez, A., Gordon, A. L., Huber, B., Castagno, P. and Falco, P.: The role of tides in bottom water export from the western Ross Sea, ~~Nature Publishing Group~~Scientific reports 1, 2021.

Boyer, T.P., O.K. Baranova, C. Coleman, H.E. Garcia, A. Grodsky, R.A. Locarnini, A.V. Mishonov, C.R. Paver, J.R. Reagan, D. Seidov, I.V. Smolyar, K. Weathers, M.M. Zweng. : World Ocean Database 2018. A.V. Mishonov, Technical Ed., NOAA Atlas NESDIS 87, 2018.

Budillon, G., Pacciaroni, M., Cozzi, S., Rivaro, P., Catalano, G., Ianni, C. and Cantoni, C.: An optimum multiparameter mixing analysis of the shelf waters in the Ross Sea, ~~Cambridge University Press~~Antarct.Sci. 1, 2003.

Bull, C. Y., Jenkins, A., Jourdain, N. C., Vaňková, I., Holland, P. R., Mathiot, P., Hausmann, U. and Sallée, J.: Remote Control of Filchner-Ronne Ice Shelf Melt Rates by the Antarctic Slope Current, ~~Wiley Online Library~~Journal of Geophysical Research: Oceans 2, 2021.

Burgard, C., Jourdain, N. C., Reese, R., Jenkins, A. and Mathiot, P.: An assessment of basal melt parameterisations for Antarctic ice shelves, The Cryosphere 12, 2022.

Cao, J., Wang, B., Yang, Y., Ma, L., Li, J., Sun, B., Bao, Y., He, J., Zhou, X. and Wu, L.: The NUIST Earth System Model (NESM) version 3: description and preliminary evaluation, ~~Copernicus GmbH~~Geoscientific Model Development 7, 2018.

Colombo, P., Barnier, B., Penduff, T., Chanut, J., Deshayes, J., Molines, J., Le Sommer, J., Verezemskaya, P., Gulev, S. and Treguier, A.: Representation of the Denmark Strait overflow in a z-coordinate eddying configuration of the NEMO (v3. 6) ocean model: resolution and parameter impacts, Geoscientific Model Development 7, 2020.

Comeau, D., Asay-Davis, X. S., Begeman, C. B., Hoffman, M. J., Lin, W., Petersen, M. R., Price, S. F., Roberts, A. F., Van Roekel, L. P. and Veneziani, M.: The DOE E3SM v1. 2 Cryosphere Configuration: Description and Simulated Antarctic Ice-Shelf Basal Melting, ~~Wiley Online Library~~Journal of Advances in Modeling Earth Systems 2, 2022.

de Lavergne, C., Vic, C., Madec, G., Roquet, F., Waterhouse, A. F., Whalen, C. B., Cuypers, Y., Bouruet-Aubertot, P., Ferron, B. and Hibiya, T.: A parameterization of local and remote tidal mixing, Journal of Advances in Modeling Earth Systems 5, 2020.

Depoorter, M. A., Bamber, J. L., Griggs, J. A., Lenaerts, J. T., Ligtenberg, S. R., van den Broeke, M. R. and Moholdt, G.: Calving fluxes and basal melt rates of Antarctic ice shelves, Nature ~~Publishing Group~~7469, 2013.

Deshayes, J., Curry, R. and Msadek, R.: CMIP5 model intercomparison of freshwater budget and circulation in the North Atlantic, J.Clim. 9, 2014.

Dufresne, J., Foujols, M., Denvil, S., Caubel, A., Marti, O., Aumont, O., Balkanski, Y., Bekki, S., Bellenger, H. and Benshila, R.: Climate change projections using the IPSL-CM5 Earth System Model: from CMIP3 to CMIP5, ~~Springer~~Clim.Dyn. 9, 2013.

Fahrbach, E., Rohardt, G., Scheele, N., Schröder, M., Strass, V. and Wisotzki, A.: Formation and discharge of deep and bottom water in the northwestern Weddell Sea, ~~Sears Foundation for Marine Research~~J.Mar.Res. 4, 1995.

Frölicher, T. L., Sarmiento, J. L., Paynter, D. J., Dunne, J. P., Krasting, J. P. and Winton, M.: Dominance of the Southern Ocean in anthropogenic carbon and heat uptake in CMIP5 models, J.Clim. 2, 2015.

Foldvik, A., Gammelsrød, T. and Tørresen, T.: Circulation and water masses on the southern Weddell Sea shelf, Oceanology of the Antarctic continental shelf, 1985.

Goosse, H., Dalaiden, Q., Cavitte, M. G. and Zhang, L.: Can we reconstruct the formation of large open-ocean polynyas in the Southern Ocean using ice core records? ~~Copernicus GmbH~~Climate of the Past 1, 2021.

Gordon, A. L. : Interocean exchange of thermocline water, ~~Wiley Online Library~~Journal of Geophysical Research: Oceans C4, 1986.

Gordon, A. L., Visbeck, M. and Huber, B.: Export of Weddell Sea deep and bottom water, ~~Wiley Online Library~~Journal of Geophysical Research: Oceans C5, 2001.

Griffies, S. M., Biastoch, A., Böning, C., Bryan, F., Danabasoglu, G., Chassignet, E. P., England, M. H., Gerdes, R., Haak, H. and Hallberg, R. W.: Coordinated ocean-ice reference experiments (COREs), ~~Elsevier~~Ocean modelling 1-2, 2009.

Harrison, L. C., Holland, P. R., Heywood, K. J., Nicholls, K. W. and Brisbourne, A. M.: Sensitivity of melting, freezing and marine ice beneath Larsen C Ice Shelf to changes in ocean forcing, ~~Wiley Online Library~~Geophys.Res.Lett. 4, 2022.

Hausmann, U., Sallée, J., Jourdain, N. C., Mathiot, P., Rousset, C., Madec, G., Deshayes, J. and Hattermann, T.: The Role of Tides in Ocean-Ice Shelf Interactions in the Southwestern Weddell Sea, ~~Wiley Online Library~~Journal of Geophysical Research: Oceans 6, 2020.

Hazeleger, W., Severijns, C., Semmler, T., Ştefănescu, S., Yang, S., Wang, X., Wyser, K., Dutra, E., Baldasano, J. M. and Bintanja, R.: EC-Earth: a seamless earth-system prediction approach in action, ~~American Meteorological Society~~Bull.Am.Meteorol.Soc. 10, 2010.

Hellmer, H. H. and Olbers, D. J.: A two-dimensional model for the thermohaline circulation under an ice shelf, ~~Cambridge University Press~~Antarct.Sci. 4, 1989.

Hellmer, H. H. : Impact of Antarctic ice shelf basal melting on sea ice and deep ocean properties, ~~Wiley Online Library~~Geophys.Res.Lett. 10, 2004.

Heuzé, C., Heywood, K. J., Stevens, D. P. and Ridley, J. K.: Southern Ocean bottom water characteristics in CMIP5 models, ~~Wiley Online Library~~Geophys.Res.Lett. 7, 2013.

Heuzé, C. : Antarctic bottom water and North Atlantic deep water in cmip6 models, ~~Copernicus GmbH~~Ocean Science 1, 2021.

Hewitt, H. T., Copsey, D., Culverwell, I. D., Harris, C. M., Hill, R., Keen, A. B., McLaren, A. J. and Hunke, E. C.: Design and implementation of the infrastructure of HadGEM3: The next-generation Met Office climate modelling system, ~~Copernicus GmbH~~Geoscientific Model Development 2, 2011.

Hewitt, H. T., Roberts, M. J., Hyder, P., Graham, T., Rae, J., Belcher, S. E., Bourdallé-Badie, R., Copsey, D., Coward, A. and Guiavarch, C.: The impact of resolving the Rossby radius at mid-latitudes in the ocean: Results from a high-resolution version of the Met Office GC2 coupled model, ~~Copernicus GmbH~~Geoscientific Model Development 10, 2016.

Holland, D. M. and Jenkins, A.: Modeling thermodynamic ice–ocean interactions at the base of an ice shelf, J.Phys.Oceanogr. 8, 1999.

Huot, P., Fichefet, T., Jourdain, N. C., Mathiot, P., Rousset, C., Kittel, C. and Fettweis, X.: Influence of ocean tides and ice shelves on ocean–ice interactions and dense shelf water formation in the D'Urville Sea, Antarctica, ~~Elsevier,~~Ocean Modelling 2021.

Hutchinson, K., Deshayes, J., Sallee, J., Dowdeswell, J. A., de Lavergne, C., Ansorge, I., Luyt, H., Henry, T. and Fawcett, S. E.: Water mass characteristics and distribution adjacent to Larsen C Ice Shelf, Antarctica, ~~Wiley Online Library~~Journal of Geophysical Research: Oceans 4, 2020.

Huthnance, J. M. : Circulation, exchange and water masses at the ocean margin: the role of physical processes at the shelf edge, ~~Elsevier~~Prog.Oceanogr. 4, 1995.

Jacobs, S. S., Gordon, A. L. and Ardai, J. L.,Jr: Circulation and melting beneath the ross ice shelf, ~~203/4379/439 [pii],~~Science, 1979.

Jacobs, S. S.: On the nature and significance of the Antarctic Slope Front, Mar.Chem. 1-4, 1991..

Janout, M. A., Hellmer, H. H., Hattermann, T., Huhn, O., Sültenfuss, J., Østerhus, S., Stulic, L., Ryan, S., Schröder, M. and Kanzow, T.: FRIS revisited in 2018: On the circulation and water masses at the Filchner and Ronne ice shelves in the southern Weddell Sea, ~~Wiley Online Library~~Journal of Geophysical Research: Oceans 6, 2021.

Jenkins, A.: A one-dimensional model of ice shelf-ocean interaction, Journal of Geophysical Research: Oceans C11, 1991.

Jeong, H., Asay-Davis, X. S., Turner, A. K., Comeau, D. S., Price, S. F., Abernathey, R. P., Veneziani, M., Petersen, M. R., Hoffman, M. J. and Mazloff, M. R.: Impacts of ice-shelf melting on water-mass transformation in the Southern Ocean from E3SM simulations, J.Clim. 13, 2020.

Johnson, G. C. : Quantifying Antarctic bottom water and North Atlantic deep water volumes, ~~Wiley Online Library~~Journal of Geophysical Research: Oceans C5, 2008.

Jourdain, N. C., Mathiot, P., Merino, N., Durand, G., Le Sommer, J., Spence, P., Dutrieux, P. and Madec, G.: Ocean circulation and sea-ice thinning induced by melting ice shelves in the Amundsen Sea, ~~Wiley Online Library~~Journal of Geophysical Research: Oceans 3, 2017.

Jourdain, N. C., Molines, J., Le Sommer, J., Mathiot, P., Chanut, J., de Lavergne, C. and Madec, G.: Simulating or prescribing the influence of tides on the Amundsen Sea ice shelves, Ocean Modelling 2019.

Kerr, R., Dotto, T. S., Mata, M. M. and Hellmer, H. H.: Three decades of deep water mass investigation in the Weddell Sea (1984–2014): temporal variability and changes, ~~Elsevier,~~Deep Sea Research Part II: Topical Studies in Oceanography 2018.

Killworth, P. D. : Deep convection in the world ocean, ~~Wiley Online Library~~Rev.Geophys. 1, 1983.

Kimmritz, M., Danilov, S. and Losch, M.: The adaptive EVP method for solving the sea ice momentum equation, ~~Elsevier,~~Ocean Modelling 2016.

Large, W. G. and Yeager, S. G.: Diurnal to decadal global forcing for ocean and sea-ice models: the data sets and flux climatologies. CGD Division of the National Center for Atmospheric Research, NCAR Technical Note: NCAR/TN-460+STR.~~ Citeseer,~~ 2004.

Lipscomb, W. H. : Remapping the thickness distribution in sea ice models, ~~Wiley Online Library~~Journal of Geophysical Research: Oceans C7, 2001.

~~Locarnini, M. M., Mishonov, A. V., Baranova, O. K., Boyer, T. P., Zweng, M. M., Garcia, H. E., Seidov, D., Weathers, K., Paver, C. and Smolyar, I.: World ocean atlas 2018, volume 1: Temperature, 2018.~~

Locarnini, M. M., Mishonov, A. V., Baranova, O. K., Boyer, T. P., Zweng, M. M., Garcia, H. E., Seidov, D., Weathers, K., Paver, C. and Smolyar, I.: World ~~ocean atlas~~Ocean Atlas 2018, volume 1: Temperature, 2018.

Locarnini, R. A., A. V. Mishonov, J. I. Antonov, T. P. Boyer, H. E. Garcia, O. K. Baranova, M. M. Zweng, C. R. Paver, J. R. Reagan, D. R. Johnson, M. Hamilton, and D. Seidov. : World Ocean Atlas 2013, 2013.

Losch, M. : Modeling ice shelf cavities in a z coordinate ocean general circulation model, ~~Wiley Online Library~~Journal of Geophysical Research: Oceans C8, 2008.

Madec, G. and NEMO System Team: Nemo ~~Ocean Engine,~~ocean engine, Scientific Notes of Climate Modelling Center (27) – ISSN 1288-1619, Institut Pierre-Simon Laplace (IPSL) 10.5281/zenodo.3878122, 2019.

~~Madec, G. and NEMO System Team: NEMO Ocean Engine, 2016.~~

Marshall, J. and Speer, K.: Closure of the meridional overturning circulation through Southern Ocean upwelling, Nature ~~Publishing Group~~Geoscience 3, 2012.

Mathiot, P., Goosse, H., Fichefet, T., Barnier, B. and Gallée, H.: Modelling the seasonal variability of the Antarctic Slope Current, ~~Copernicus GmbH~~Ocean Science 4, 2011.

Mathiot, P., Jenkins, A., Harris, C. and Madec, G.: Explicit representation and parametrised impacts of under ice shelf seas in the $z*$ coordinate ocean model NEMO 3.6, ~~Copernicus GmbH~~Geoscientific Model Development 7, 2017.

Mazloff, M. R., Heimbach, P. and Wunsch, C.: An eddy-permitting Southern Ocean state estimate, ~~American Meteorological Society~~J.Phys.Oceanogr. 5, 2010.

~~Melsheimer, C. and Spreen, G.: AMSR-E ASI sea ice concentration data, Antarctic, version 5.4 (NetCDF) (June 2002 - September 2011), https://doi.pangaea.de/10.1594/PANGAEA.919778, 2020.~~

Menviel, L., Timmermann, A., Timm, O. E. and Mouchet, A.: Climate and biogeochemical response to a rapid melting of the West Antarctic Ice Sheet during interglacials and implications for future climate, ~~Wiley Online Library~~Paleoceanography 4, 2010.

Meredith, M., Sommerkorn, M., Cassotta, S., Derksen, C., Ekaykin, A., Hollowed, A., Kofinas, G., Mackintosh, A., Melbourne-Thomas, J., Muelbert, M.M.C. and Ottersen, G. : Polar regions. IPCC Special Report on the Ocean and Cryosphere in a Changing Climate, ~~https://www. ipcc.~~ IPCC https://www.ipcc.ch/srocc/chapter, p.2., 2019.

Merino, N., Le Sommer, J., Durand, G., Jourdain, N. C., Madec, G., Mathiot, P. and Tournadre, J.: Antarctic icebergs melt over the Southern Ocean: Climatology and impact on sea ice, ~~Elsevier~~Ocean Modelling, 2016.

Moholdt, G., Padman, L. and Fricker, H. A.: Basal mass budget of Ross and Filchner-Ronne ice shelves, Antarctica, derived from Lagrangian analysis of ICESat altimetry, ~~Wiley Online Library~~Journal of Geophysical Research: Earth Surface 11, 2014.

Mohrmann, M., Heuzé, C. and Swart, S.: Southern Ocean polynyas in CMIP6 models, ~~Copernicus GmbH~~The Cryosphere 9, 2021.

Nakayama, Y., Timmermann, R. and H Hellmer, H.: Impact of West Antarctic ice shelf melting on Southern Ocean hydrography, ~~Copernicus GmbH~~The Cryosphere 7, 2020.

Naughten, K. A., Meissner, K. J., Galton-Fenzi, B. K., England, M. H., Timmermann, R., Hellmer, H. H., Hattermann, T. and Debernard, J. B.: Intercomparison of Antarctic ice-shelf, ocean, and sea-ice interactions simulated by MetROMS-iceshelf and FESOM 1.4, ~~Copernicus GmbH~~Geoscientific Model Development 4, 2018.

Naughten, K. A., De Rydt, J., Rosier, S. H., Jenkins, A., Holland, P. R. and Ridley, J. K.: Two-timescale response of a large Antarctic ice shelf to climate change, Nature ~~Publishing Group~~communications 1, 2021.

Naveira Garabato, A. C., McDonagh, E. L., Stevens, D. P., Heywood, K. J. and Sanders, R. J.: On the export of Antarctic bottom water from the Weddell Sea, ~~Elsevier~~Deep Sea Research Part II: Topical Studies in Oceanography 21, 2002.

NEMO System Team~~.~~: NEMO ocean engine, scientific notes of climate modelling center, 27, ISSN 1288-1619 Institut Pierre-Simon Laplace (IPSL), ~~Institut Pierre-Simon Laplace (IPSL), Paris,~~ 10.5281/zenodo.~~1464816~~6334656, 2022.

Nicholls, K. W., Østerhus, S., Makinson, K. and Johnson, M. R.: Oceanographic conditions south of Berkner Island, beneath Filchner-Ronne Ice Shelf, Antarctica, ~~Wiley Online Library~~Journal of Geophysical Research: Oceans C6, 2001.

Nicholls, K. W., Pudsey, C. J. and Morris, P.: Summertime water masses off the northern Larsen C Ice Shelf, Antarctica, ~~Wiley Online Library~~Geophys.Res.Lett. 9, 2004.

Nicholls, K. W., Østerhus, S., Makinson, K., Gammelsrød, T. and Fahrbach, E.: Ice-ocean processes over the continental shelf of the southern Weddell Sea, Antarctica: A review, ~~Wiley Online Library~~Rev.Geophys. 3, 2009.

NOAA~~.~~: National Geophysical Data Center 2-minute gridded global relief data (ETOPO2) v2, ~~2006.~~National Geophysical Data Center NOAA, 2006.

Orsi, A. H., Johnson, G. C. and Bullister, J. L.: Circulation, mixing, and production of Antarctic Bottom Water, ~~Elsevier~~Prog.Oceanogr. 1, 1999.

Orsi, A. H. : Recycling bottom waters, Nature ~~Publishing Group~~Geoscience 5, 2010.

Phipps, S. J., Fogwill, C. J. and Turney, C. S.: Impacts of marine instability across the East Antarctic Ice Sheet on Southern Ocean dynamics, ~~Copernicus GmbH~~The Cryosphere 5, 2016.

Prather, M. J. : Numerical advection by conservation of second-order moments, ~~Wiley Online Library~~Journal of Geophysical Research: Atmospheres D6, 1986.

Rignot, E., Jacobs, S., Mouginot, J. and Scheuchl, B.: Ice-shelf melting around Antarctica, ~~American Association for the Advancement of~~ Science 6143, 2013.

Rintoul, S. R~~. :~~.: The global influence of localized dynamics in the Southern Ocean, Nature ~~Publishing Group~~7709, 2018.

Robertson, R., Visbeck, M., Gordon, A. L. and Fahrbach, E.: Long-term temperature trends in the deep waters of the Weddell Sea, ~~Elsevier~~Deep Sea Research Part II: Topical Studies in Oceanography 21, 2002.

Rohardt, G., Fahrbach, E., Beszczynska-Möller, A., Boetius, A., Brunßen, J., Budéus, G., Cisewski, B., Engbrodt, R., Gauger, S., Geibert, W., Geprägs, P., Gerdes, D., Gersonde, R., Gordon, A. L., Hellmer, H. H., Isla, E., Jacobs, S. S., Janout, M. A., Jokat, W., Klages, M., Kuhn, G., Meincke, J., Ober, S., Østerhus, S., Peterson, R. G., Rabe, B., Rudels, B., Schauer, U., Schröder, M., Sildam, J., Soltwedel, T., Stangeew, E., Stein, M., Strass, V. H., Thiede, J., Tippenhauer, S., Veth, C., von Appen, W., Weirig, M., Wisotzki, A., Wolf-Gladrow, D. A. and Kanzow, T.: Physical oceanography on board of POLARSTERN (1983-11-22 to 2016-02-14). Alfred Wegener Institute, Helmholtz Centre for Polar and Marine Research, Bremerhaven, 10.1594/PANGAEA.860066, 2016.

Sallée, J., Pellichero, V., Akhoudas, C., Pauthenet, E., Vignes, L., Schmidtko, S., Garabato, A. N., Sutherland, P. and Kuusela, M.: Summertime increases in upper-ocean stratification and mixed-layer depth, Nature ~~Publishing Group~~7851, 2021.

Scoccimarro, E., Gualdi, S., Bellucci, A., Sanna, A., Giuseppe Fogli, P., Manzini, E., Vichi, M., Oddo, P. and Navarra, A.: Effects of tropical cyclones on ocean heat transport in a high-resolution coupled general circulation model, J.Clim. 16, 2011.

Siahaan, A., Smith, R., Holland, P., Jenkins, A., Gregory, J. M., Lee, V., Mathiot, P., Payne, T., Ridley, J. and Jones, C.: The Antarctic contribution to 21st century sea-level rise predicted by the UK Earth System Model with an interactive ice sheet, ~~Copernicus GmbH~~The Cryosphere Discussions, 2021.

Silvano, A., Rintoul, S. R. and Herraiz-Borreguero, L.: Ocean-ice shelf interaction in East Antarctica, Oceanography 4, 2016.

Silvano, A., Rintoul, S. R., Peña-Molino, B., Hobbs, W. R., van Wijk, E., Aoki, S., Tamura, T. and Williams, G. D.: Freshening by glacial meltwater enhances melting of ice shelves and reduces formation of Antarctic Bottom Water, Science advances 4, 2018.

Smethie Jr, W. M. and Jacobs, S. S.: Circulation and melting under the Ross Ice Shelf: estimates from evolving CFC, salinity and temperature fields in the Ross Sea, ~~Elsevier~~Deep Sea Research Part I: Oceanographic Research Papers 6, 2005.

Smith, R. S., Mathiot, P., Siahaan, A., Lee, V., Cornford, S. L., Gregory, J. M., Payne, A. J., Jenkins, A., Holland, P. R. and Ridley, J. K.: Coupling the UK Earth System Model to dynamic models of the Greenland and Antarctic ice sheets, ~~Wiley Online Library~~Journal of Advances in Modeling Earth Systems 10, 2021.

~~Solodoch, A., Stewart, A. L., Hogg, A. M., Morrison, A. K., Kiss, A. E., Thompson, A. F., Purkey, S. G. and Cimoli, L.: How Does Antarctic Bottom Water Cross the Southern Ocean? Wiley Online Library, 2022.~~

Solodoch, A., Stewart, A. L., Hogg, A. M., Morrison, A. K., Kiss, A. E., Thompson, A. F., Purkey, S. G. and Cimoli, L.: How Does Antarctic Bottom Water Cross the Southern Ocean? ~~Wiley Online Library~~Geophys.Res.Lett. 7, 2022.

Storkey, D., Blaker, A. T., Mathiot, P., Megann, A., Aksenov, Y., Blockley, E. W., Calvert, D., Graham, T., Hewitt, H. T. and Hyder, P.: UK Global Ocean GO6 and GO7: A traceable hierarchy of model resolutions, ~~Copernicus GmbH~~Geoscientific Model Development 8, 2018.

Swart, N. C., Cole, J. N., Kharin, V. V., Lazare, M., Scinocca, J. F., Gillett, N. P., Anstey, J., Arora, V., Christian, J. R. and Hanna, S.: The Canadian earth system model version 5 (CanESM5. 0.3), ~~Copernicus GmbH~~Geoscientific Model Development 11, 2019.

Thompson, A. F., Stewart, A. L., Spence, P. and Heywood, K. J.: The Antarctic Slope Current in a changing climate, ~~Wiley Online Library~~Rev.Geophys. 4, 2018.

van~~Vancoppenolle, M., Rousset, C., Blockley, E., and the NEMO Sea Ice Working Group: SI3 – Sea Ice modelling Integrated Initiative – The NEMO Sea Ice Engine, 10.5281/zenodo.7534900, 2023.~~

~~Van~~ Caspel, M., Schröder, M., Huhn, O. and Hellmer, H. H.: Precursors of Antarctic Bottom Water formed on the continental shelf off Larsen Ice Shelf, ~~Elsevier~~Deep Sea Research Part I: Oceanographic Research Papers, 2015.

Vancoppenolle, M., Rousset, C., Blockley, E., and the NEMO Sea Ice Working Group. : SI3 – Sea Ice modelling Integrated Initiative – The NEMO Sea Ice Engine, 10.5281/zenodo.7534900, 2023.

Voldoire, A., Sanchez-Gomez, E., Salas y Mélia, D., Decharme, B., Cassou, C., Sénési, S., Valcke, S., Beau, I., Alias, A. and Chevallier, M.: The CNRM-CM5. 1 global climate model: description and basic evaluation, ~~Springer~~Clim.Dyn. 9, 2013.

Whitehead, J. A. : Dense water off continents, Nature ~~Publishing Group~~6124, 1987.

Williams, G. D., Herraiz-Borreguero, L., Roquet, F., Tamura, T., Ohshima, K. I., Fukamachi, Y., Fraser, A. D., Gao, L., Chen, H. and McMahon, C. R.: The suppression of Antarctic bottom water formation by melting ice shelves in Prydz Bay, Nature Communications 1, 2016.

Zweng, M. M., Seidov, D., Boyer, T. P., Locarnini, M., Garcia, H. E., Mishonov, A. V., Baranova, O. K., Weathers, K., Paver, C. R. and Smolyar, I.: World ~~ocean atlas~~Ocean Atlas 2018, volume 2: Salinity, 2019.

Zweng, M.M, J.R. Reagan, J.I. Antonov, R.A. Locarnini, A.V. Mishonov, T.P. Boyer, H.E. Garcia, O.K. Baranova, D.R. Johnson, D.Seidov, M.M. Biddle. : World Ocean Atlas 2013, 2013.

# Supplementary Material

**Formatted:** Font: 15 pt

## S1 A note on the NEMO namelists

In the Zenodo data repository associated with this manuscript (10.5281/zenodo.7561767), the NEMO reference namelist (namelist_ref), “Open” configuration namelist  (namelist_core_ia_cfg) and sea ice namelists (namelist_ice_ref and namelist_ice_cfg) are given. The reference namelist is the default provided with the NEMO code. Unless stated otherwise in the “cfg”, the simulation uses the choices selected in the “ref” namelist. The namelist_core_ia_cfg is specific to a global ocean configuration (with modifications adapted to eORCA1) forced by interannual core winds. For more information on all the parameters included in these namelists, please refer to the NEMO reference manual available on Zenodo (10.5281/zenodo.6334656). Of specific interest may be Chapter 6.10 on “Interaction with ice shelves (ISF)” where the various options to represent ice-shelf/ ocean fluxes, heat and salt exchange coefficients and melt parameterization choices are explained.

The differences in namelist_core_ia_cfg for the “Open” and “Closed” cavity runs are listed in Table S1. Note that these differences are minor as the adaptations are made mostly to the input files (explained under “DOMAIN FILES AND INITIAL CONDITIONS” in Zenodo data repository description 10.5281/zenodo.7561767).

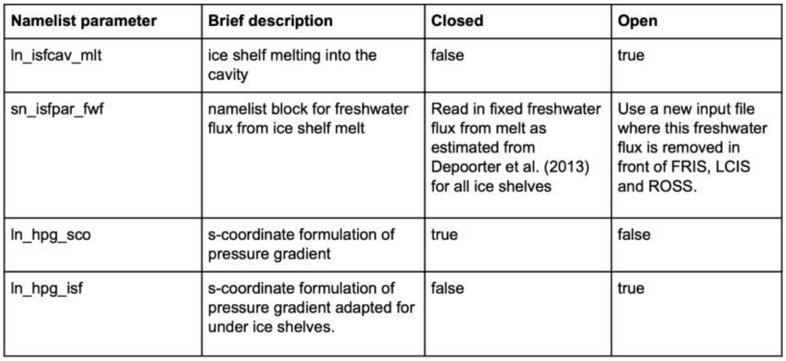

| Namelist parameter | Brief description | Closed | Open |
|---|---|---|---|
| ln_isfcav_mlt | ice shelf melting into the cavity | false | true |
| sn_isfpar_fwf | namelist block for freshwater flux from ice shelf melt | Read in fixed freshwater flux from melt as estimated from Depoorter et al. (2013) for all ice shelves | Use a new input file where this freshwater flux is removed in front of FRIS, LCIS and ROSS. |
| ln_hpg_sco | s-coordinate formulation of pressure gradient | true | false |
| ln_hpg_isf | s-coordinate formulation of pressure gradient adapted for under ice shelves. | false | true |

Table S1 Namelist differences when FRIS, LCIS and ROSS cavities are open.

## S2 An alternative methodology to parameterize the effect of tides under the ice shelves

### S2.1 Rationale

The influence of tides on ice shelf basal melt is parameterized in NEMO using a constant background kinetic energy, set to the value of 2.5 x $10^{-3}$ $m^2$ $s^{-2}$ everywhere (namelist parameter rn_ke0). As discussed in Jourdain et al. (2019), within ice shelf cavities tides play an important role in modulating basal melt by imposing an added current velocity along the ice shelf base. The magnitude of the tidal currents are, however, not constant everywhere, and so a single kinetic energy value (as is the default option in NEMO) can be improved upon by using a two dimensional field. To inform this, we follow the methodology of Jourdain et al. (2019) and use the Circum-Antarctic Tidal Simulation CATS2008 tidal map interpolated onto the eORCA1 grid (Howard et al., 2019). Additionally, some of the NEMO code had to be adapted to allow for this type of tidal parameterization and so the following files were amended: isf_oce.F90, isfcavgam.F90, isfstp.F90, zdfdrg.F90. The simulation was run for 124 years and the differences in melt rate between this simulation and the reference “Open” cavity simulation are presented in Fig. S1.

### S2.2 Impact of alternative tidal parameterization on basal melt

Using the two-dimensional CATS tidal atlas to parameterize the effect of tides slightly increases melt for FRIS (total mean melt flux over 1995-2009 of 120 ± 22 Gt/yr) and LCIS (39 ± 8 Gt/yr) and reduces net melt for ROSS (102 ± 18 Gt/yr) compared to results shown in Table 1. In general, the tidal velocities for CATS under FRIS and LCIS are faster than the default constant and for RIS are slower. The spatial differences in yearly basal melt rate can be seen in Fig. S1. The marked differences for FRIS are an increase in melt at the ice shelf front and a decrease within the deep fjords along the grounding line. An explanation for this is that the elevated tidal velocities increase the rate of melting as warm offshore water enters the cavity, causing elevated melt along the western ice shelf front. This water then loses its heat, and thus potential for melt, and slows down as it travels into the southernmost extremities of the cavity where it induces less melt than in the default simulation. The converse is true for RIS where the CATS tidal map shows slower induced velocities than the default parameterization, meaning a decrease in the melt rate all along the ice shelf front. To explore the impact of these changes in melt rate on water mass properties, we also compared with two cross sections across the ice shelf fronts (FRIS February 1995 and RIS February 2000) and found temperature differences of less than 0.1°C and salinity differences of less than 0.05 psu using this alternative method to represent the tidal effect. These plots are not included here as it is impossible to see the difference compared to Figs. 6 and 7 with the naked eye, and another anomaly plot adds no value to the reader.

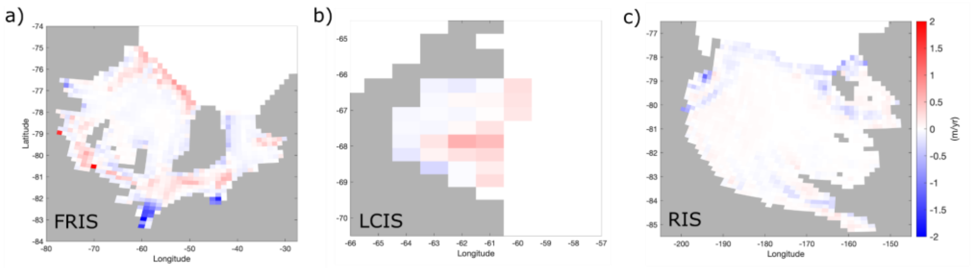

Figure S1. Difference in melt rates (CATS tides - default parameterization) for (a) Filchner-Ronne Ice Shelf, (b) Larsen C Ice Shelf and (c) Ross Ice Shelf. The results are mean values for the model equivalent period 1995-2009. A positive difference indicates more melting for the "CATS tides" run in areas of melt in Figure 4, and less freezing in areas of re-freezing in Figure 4.

### S2.3 Conclusion

This simulation using a two dimensional map of tidal velocities informed by CATS2008 shows minor changes in net melt flux for each cavity (<10 Gt/yr) and small adjustments in the melt rate pattern (<2 m/yr). These changes are not as large as one would expect when tides are explicitly simulated as in that case, the basin wide circulation and water mass distribution would be affected. Explicit tides were not explored in this study as the eORCA1 configuration we use is designed for climate applications (explicit tides do not fit this purpose as they contribute too much numerical mixing).

## S3 An evaluation of sea ice production and polynya activity in the NEMO simulations

In this section, we analyze polynya activity in the Ronne and Ross polynya regions and explore corresponding changes when FRIS and RIS cavities are opened.

### S3.1 Polynya realism in the NEMO simulation without cavities

Ice production in the Ronne and Ross polynya regions in the present NEMO v4.2 eORCA1 configuration is found to overall align well with observed coastal patterns. 'Ice production' is diagnosed as the annual integral of sea ice generated over a domain spanning 73-80 °S and 30-60 °W for the Ronne Polynya region, and 160 °E to 155 °W south of 74 ºS for the Ross Polynya region. When FRIS melt is parameterized ("Closed" run), the Ronne Polynya region produces 24 x $10^9$ $m^3$ of ice per year, compared to 58 ± 21 x $10^9$ $m^3$ reported from the satellite-based estimates of Nakata et al (2021). The Ross Polynya region produces 368 x $10^9$ $m^3$ of ice per year in the "Closed" simulation, compared to 387 ± 41 x $10^9$ $m^3$ reported in Nakata et al (2021). It is important to note here that model output and satellite-based estimates are not directly comparable due to differing definitions for the region of interest between the two sources. If we look at the patterns of sea ice production (Fig. S2), we see the largest values of around 5 m $yr^{-1}$ at the expected locations along the coasts of Antarctica (Nakata et al 2021). Terra Nova Bay Polynya does not correspond exactly to the observed position, likely due to the absence of simulated landfast sea ice.

## S3.2 Impact of explicit sub-ice shelf circulation on polynya activity

The changes in polynya activity in response to opening FRIS and RIS are minor. We find no change in the location of polynyas. Ice production does, however, slightly increase from 24 to 29 x $10^9$ $m^3$ in the Ronne Polynya region and slightly decrease from 368 to 357 x $10^9$ $m^3$ in the Ross Polynya region. Ice production slightly decreases to the west of the ice shelf fronts and increases eastward in both analyzed regions when cavities are opened, with changes smaller than 0.5 m $yr^{-1}$. Changes in ice production are consistent with simulated temperature shifts, with warming to the west and cooling to the east of FRIS and RIS (see Figs. 2 and 3) in the "Open" cavity simulation. Due to the very minor changes in volume of ice production and the absence of a location shift in polynyas, the volume of HSSW produced in each simulation is comparable. The majority of the salinity alterations observed in Figures 2i and 3i are thus likely driven by a change in circulation patterns when the paths under the ice shelf are opened and not by an alteration in volume of HSSW produced from polynya activity.

**Formatted:** Space Before: 12 pt, After: 12 pt

**Formatted:** Font: 10 pt, Not Bold

**Formatted:** Font: 10 pt, Not Bold

## S3.3 Summary

In summary, sea ice production is reasonable for the two large polynya regions we resolve (Ronne & Ross). Changes in polynya activity due to the opening of the sub-ice shelf cavities can be explained as a response to adjustments in temperature patterns. In conclusion, these effects are minor, do not change the overall locations of the polynyas, and the feedback of sea ice changes on water properties is considered weak.

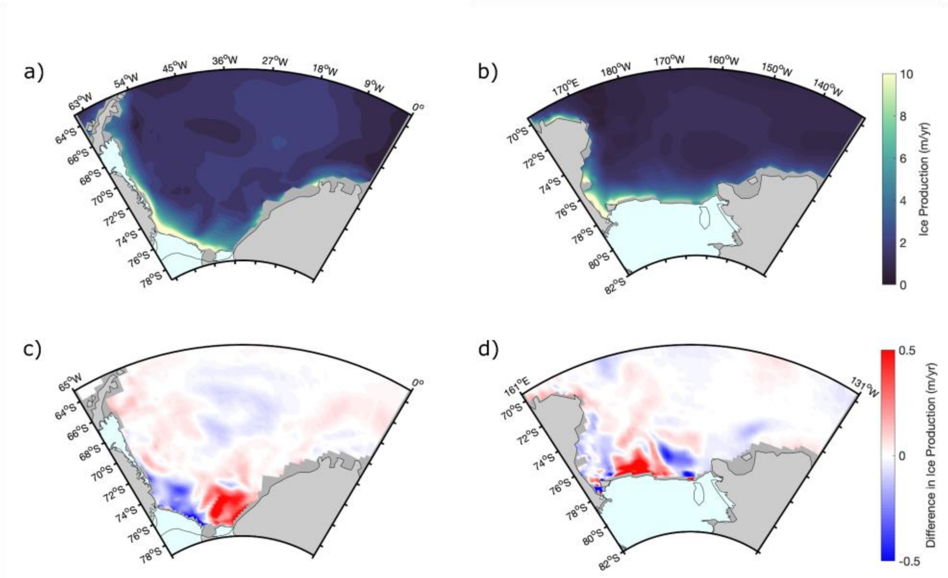

Figure S2: The annual mean sea ice production in NEMO "Closed" configuration for (a) the Weddell Sea and (b) the Ross Sea. The difference in ice production between the "Open" and "Closed" cavity runs (Open-Closed) are shown in plots (c) and (d) for Weddell and Ross seas respectively.

**Data availability:**

CATS2008 is available for download through the U.S. Antarctic Program Data Center: Data DOI: 10.15784/601235

**References:**

Howard, S., Padman, L. and Erofeeva, S.: Cats2008: Circum-antarctic tidal simulation version 2008, United States Antarctic Program Data Center 2019.

Jourdain, N. C., Molines, J., Le Sommer, J., Mathiot, P., Chanut, J., de Lavergne, C. and Madec, G.: Simulating or prescribing the influence of tides on the Amundsen Sea ice shelves, Ocean Modelling 2019.

Nakata, K., Ohshima, K. I. and Nihashi, S.: Mapping of active frazil for Antarctic coastal polynyas, with an estimation of sea-ice production, Geophys.Res.Lett. 6, 2021.

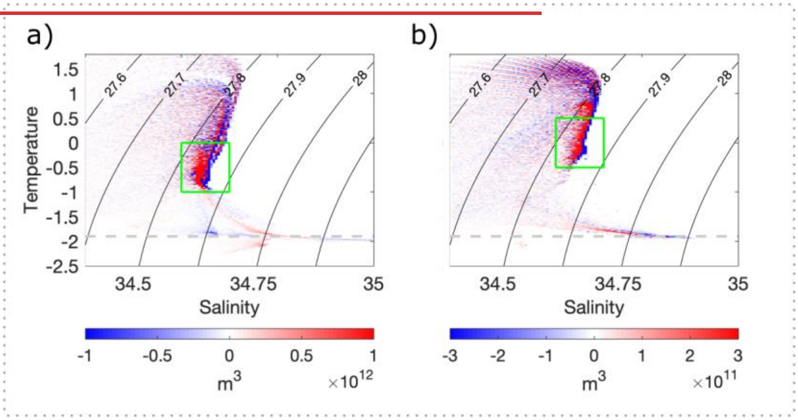

# Supplementary ~~figure 1~~Figures

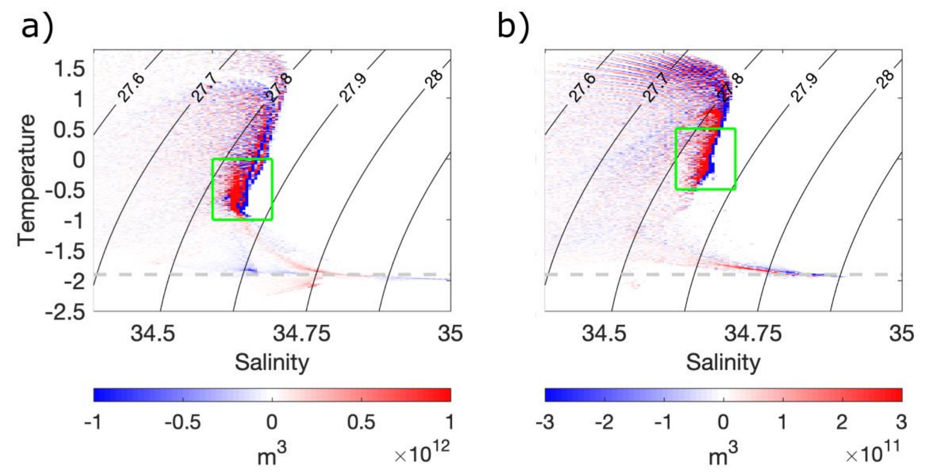

Figure S3: Difference ("Open" - "Closed") in volumetric temperature versus salinity distributions for (a) the Weddell Sea (80°S-60°S ; 65°W-20°E) and (b) the Ross Sea (85°S-68°S; 130°W-160°E) for model output excluding data underneath the ice shelves. The scatter dots are placed in T-S space according to their position in the "Closed" cavity simulation and the coloring shows the "Open"-"Closed" volumetric difference. The green boxes delimit the properties corresponding to AABW.

**Formatted:** Font: 15 pt

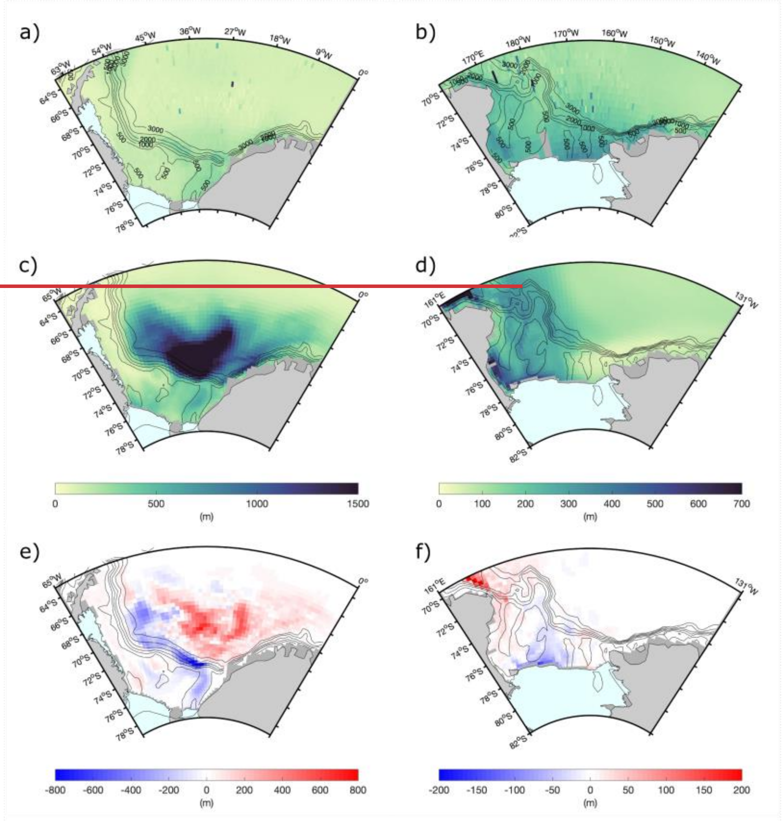

~~Supplementary Fig. 2: Winter mixed layer depths (MLD) from observational atlas of Sallee et al. (2021) shown in (a) and (b) for the Weddell and Ross Sea respectively, are compared with the winter mean from NEMO v4.2 eORCA1 forced model reference configuration equivalent years 1971-2009 in (c) and (d). The differences in MLDs between the "Open" cavity run and reference "Closed" run are shown in subplots (e) and (f).~~

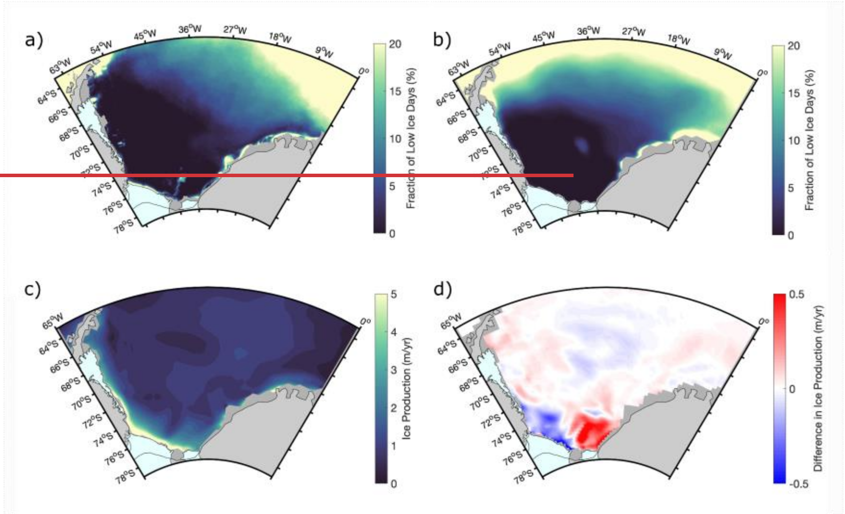

~~Supplementary Fig. 3: The fraction of low ice days for the period 2003-2009 for (a) satellite AMSR observations (Melsheimer et al., 2020) and (b) the NEMO "Closed" cavity reference configuration. Plot (c) shows the annual mean ice production in NEMO "Closed" configuration and (d) shows the~~

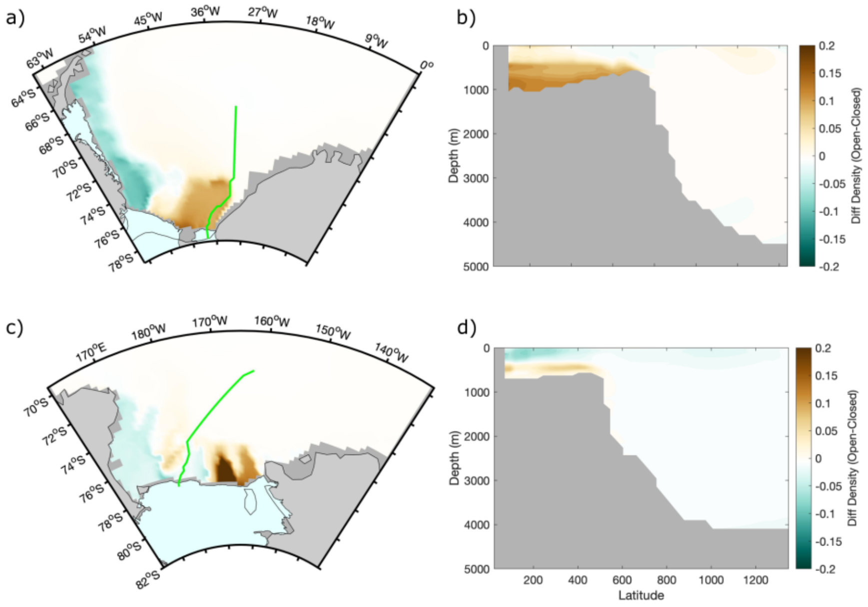

Figure S4: Density difference ~~in ice production between the "Open" and "Closed" cavity run (Open-Closed).~~

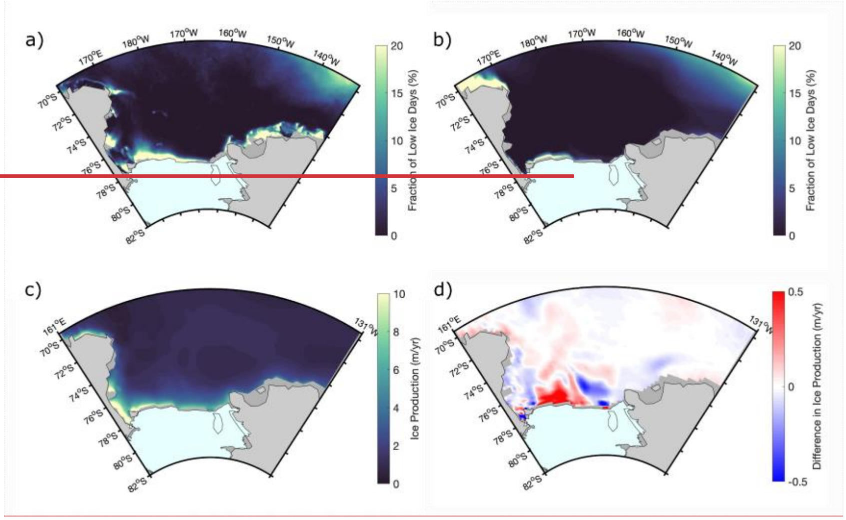

~~Supplementary Fig. 4: Same as S3 but for the Ross Sea~~

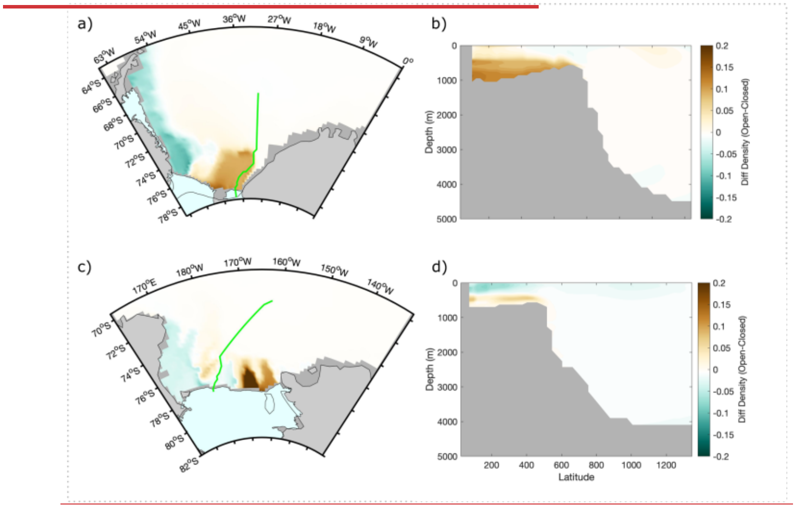

~~Supplementary Fig. 5: Density~~ (kg~~/m3~~ m$^{-3}$) plots for the Weddell (a-b) and Ross (c-d) Seas with bottom ~~density~~values in subplots (a) and (c) and the cross sections of the Filchner and Challenger troughs illustrated by green lines shown in subplots (b) and (d).

# ~~Supplementary Material~~

### ~~S1 An evaluation of ice production and polynya activity in the NEMO simulations~~

### ~~S1.1 Scope~~

~~Sea ice growth, melt and drift exert an influence on water mass properties, according to many observational and model studies. In particular, near the Ronne and Ross ice shelf margins of interest for this study, during the cold season, large polynyas source dense saline waters to the surface ocean. In this Supplementary Material, we provide an evaluation of polynya activity in these two locations from our simulations and address: (i) how realistic polynya activity is; (ii) how polynya activity changes in response to the opening of cavities; and (iii) how associated changes in polynya activity affect biases in simulated water mass properties.~~

### ~~S1.2 Methods~~

~~As an observational basis, we use the daily ice concentration 6.25 km resolution AMSR-E ASI product (Melsheimer and Spreen, 2020), best suited to the study of polynyas with its high resolution and daily coverage. From this, following Massom et al (1998), we diagnose annual polynya activity from the *fraction of low-ice days*, namely the fraction of days with ice concentration < 75 % over a 180-day period (days 91-270, i.e. April-September). From annual values, we compute the 2003-2009 mean, mapped in Figs. S3a and S4a for Weddell and Ross Sea regions, respectively.~~

~~We compute a comparable diagnostic from model daily ice concentration outputs, whose 2003-2009 average in the “Closed” simulation is mapped in Figs. S3b and S4b.~~

~~We supplement these diagnostics with simulated annual ice production, computed as the total volume of ice produced per unit area each year. Figs. S3c and S4c map 2003-2009 averages for the “Closed” simulation and Figs. S3d and S4d show the “Open”-”Closed” difference.~~

~~We also calculate yearly ice production summed over each polynya region and compare the results with observational counterparts in the Supplementary Table below.~~

| ~~Ice production ($10^9$ m$^3$)~~ | ~~Nakata et al. (2021)~~ | ~~Closed~~ | ~~Open~~ |
|---|---|---|---|
| ~~Ronne Polynya~~ | ~~58 ± 21~~ | ~~24~~ | ~~29~~ |
| ~~Ross + Terra Nova Bay Polynya~~ | ~~387 ± 41~~ | ~~368~~ | ~~357~~ |

~~Supplementary table 1: Comparison between observational estimates and the NEMO eORCA1 configuration “Closed” and “Open” cavity runs for net ice production in Ronne Polynya of the Weddell Sea and the sum of Ross and Terra Nova Bay polynyas of the Ross Sea.~~

### ~~**S1.4 Evaluating polynya activity**~~

~~The observed fraction of low ice days indicates polynya activity at the expected locations (see, e.g., Nakata et al, 2021). In the Weddell Sea, this includes the Ronne Polynya off Ronne Ice Shelf (Fig. S3a); in the Ross Sea, this includes the Ross and Terra Nova Bay polynyas (Fig. S4a) and smaller polynyas further north. This corresponds to where we observe hyper-saline bottom waters (Figs. 2f and 3f).~~

~~Unlike observations, the simulated fraction of low ice days shows no apparent polynya activity along the ice-shelf fronts (Figs. S3b and S4b). We argue that this discrepancy is due to inconsistencies between the way the model and observations define ice concentration. Indeed, in the model, sea ice drift (aka *dynamics*), then growth and melt (aka *thermodynamics*) are calculated sequentially, at each time step. In this context, any dynamically-driven opening in the ice is, under the action of sufficiently cold air, instantaneously frozen by model thermodynamics, with thin ice. Such thin ice contributes to ice concentration as ice of any thickness, explaining why simulated concentration can be nearly 100 % in polynya regions. Satellite retrievals of ice concentration possess inherent differences with model estimates. First they have much higher resolution. Second, they contrast thick ice and open water fairly well and do not suffer from the closing effect described above. All this contributes to lower ice concentration in polynya regions in satellite products as compared with NEMO output. An additional contributing factor might be that thin ice and open water are hard to distinguish, such that some thin ice might be counted as open water in satellite products, as has been shown to occur for at least some sea ice passive microwave (PMW) algorithms (Kern et al., 2022).~~

~~From simulated ice production, Ronne (Fig. S3c), Ross and Terra Nova Bay (Fig. S4c) polynyas have a clear signature in the model, at the approximate locations inferred from the observed low-ice-day fraction. Fairly similar patterns are seen in simulated ice thickness fields (not shown), with very thin (<25 cm) ice found where polynas are deemed active. For these reasons, we surmise that there are active polynyas in our simulations, but that the fraction of low-ice days is a poor diagnostic for their identification. Instead, ice production captures the polynya activity and most importantly reflects their impact on water-mass transformation.~~

~~Annual ice production maps also indicate possible errors in the distribution of simulated polynya activity. In particular, the Ross Sea Polynya seems too narrow, whereas the Terra Nova Bay polynya seems too wide, especially north of McMurdo Sound, possibly due to the lack of landfast ice in the simulations north of McMurdo Sound (Fraser et al., 2021).~~

~~Annually-integrated ice production in the Ronne Polynya under-estimates observations. By contrast, ice production in the Ross and Terra Nova Bay polynyas is consistent with the observational estimate, though the simulated production rate is based on too large an area.~~

### ~~**S1.5 Effect of opening cavities on polynya activity**~~

~~Opening cavities is associated with changes in ice production close to the polynya regions. Overall, the annually integrated ice production (Supplementary Table 1) only slightly changes because the net effect is a residual between roughly equal~~

~~areas of ice production decrease (to the west of the ice shelves) and increase (to the east of the ice shelves). It is hard to conclude on more or less realistic polynya activity in the “Open” simulation.~~

~~Changes in ice production due to opening cavities are largely consistent with patterns of temperature and salinity adjustments. Ice production is lower where temperature is higher and salinity is lower. This is consistent with circulation-induced ocean temperature changes forcing an alteration in ice production, with possible feedback on salinity. In the Weddell Sea, a re-organisation of the shelf circulation to subduct HSSW under the ice shelf reduces the ice production in the Ronne Depression and increases it to the east over the Filchner Trough. The pattern of sea ice change in the Ross Sea is less homogeneous east-west, with a reduction in Terra Nova Bay and in front of Roosevelt Island and an increase in sea ice over the Challenger Trough which is where ice shelf water (ISW) is exported.~~

## ~~S1.6 Summary~~

~~In summary, ice production in polynya regions decreases west of the ice shelves and mostly increases east of them when opening cavities. The decrease to the west may contribute to a reduction of the high salinity bias there. On the eastern side, increased ice production and brine rejection combines with northward export of cold ISW from the under-ice cavities. The resultant effect in the Weddell Sea is a strong east-west temperature and salinity difference (Fig. 2i). In the Ross Sea, on the other hand, increased brine rejection seems compensated by anomalous export of relatively fresh water from under the ice shelf (Fig. 3i).~~

## ~~Data~~

~~The AMSR-E ASI sea ice concentration data used can be found at: https://doi.pangaea.de/10.1594/PANGAEA.919778~~

## ~~Bibliography~~

~~Nakata, K., Ohshima, K. I. and Nihashi, S.: Mapping of active frazil for Antarctic coastal polynyas, with an estimation of sea-ice production, Wiley Online Library, 2021.~~

~~Melsheimer, C. and Spreen, G.: AMSR-E ASI sea ice concentration data, Antarctic, version 5.4 (NetCDF) (June 2002 – September 2011), https://doi.pangaea.de/10.1594/PANGAEA.919778, 2020.~~

~~Massom, R. A., Harris, P. T., Michael, K. J. and Potter, M. J.: The distribution and formative processes of latent-heat polynyas in East Antarctica, Cambridge University Press, 1998.~~

~~Fraser, A. D., Massom, R. A., Handcock, M. S., Reid, P., Ohshima, K. I., Raphael, M. N., Cartwright, J., Klekociuk, A. R., Wang, Z. and Porter-Smith, R.: Eighteen-year record of circum-Antarctic landfast-sea-ice distribution allows detailed baseline characterisation and reveals trends and variability, Copernicus GmbH, 2021.~~

~~Kern, S., Lavergne, T., Pedersen, L. T., Tonboe, R. T., Bell, L., Meyer, M. and Zeigermann, L.: Satellite passive microwave sea-ice concentration data set intercomparison using Landsat data, Copernicus GmbH, 2022.~~